UNIVERSITY OF
GOTHENBURG

THESIS FOR THE DEGREE OF DOCTOR OF PHILOSOPHY

Structure-Specific Vibrational Modes of Isolated Biomolecules Studied with Mid- and Far-Infrared Laser Spectroscopy

Author:
Vasyl YATSYNA

Supervisor:
Dr. Vitali Zhaunerchyk

Co-supervisors:
Dr. Anouk M. Rijs
Prof. Raimund Feifel

Examiner:
Prof. Dag Hanstorp

Department of Physics
University of Gothenburg
Gothenburg, Sweden 2019

Doctoral Dissertations in Physics

Department of Physics
University of Gothenburg
412 96 Gothenburg, Sweden

January 14, 2019

ISBN: 978-91-7833-296-0 (print)
ISBN: 978-91-7833-297-7 (pdf)
URL: http://hdl.handle.net/2077/58138

Cover: Artistic impression of laser spectroscopy of isolated biomolecules. Molecules are excited with infrared laser light, which cause them to vibrate. Yellow arrows show several kinds of vibrational motions ("dances"), that the depicted Ala-Ala peptide molecule can perform in the mid- and far-infrared frequency ranges. The ultraviolet laser ionizes only those molecules that were not excited by the infrared laser.

Printed by BrandFactory, Kållered, 2019

Typeset using LaTeX

Abstract

Biomolecular structure elucidation is crucial for our detailed understanding of various biological processes, since there is an intimate relationship between the biomolecular function and structure. In this respect, isolated biomolecules, despite being outside of their natural environment, are perfect model systems for in-depth studies of various fundamental interactions that govern the formation of biomolecular structure. This thesis focuses on structure elucidation of isolated molecules of biological importance, with special emphasis on the development of novel infrared (IR) laser spectroscopic tools.

The first part of the thesis applies far-IR spectroscopy, which excites low-frequency molecular vibrations in the IR light wavelength range of $\lambda > 12$ μm. The far-IR range provides valuable structural information complementing the well-established mid-IR ($\lambda = 2.5-12$ μm) spectroscopic analysis. However, routine application of far-IR spectroscopy to biomolecular structure elucidation is complicated by the limited knowledge of structure-specific far-IR spectral features, as well as poor performance of conventional theoretical approaches for the treatment of delocalized and anharmonic far-IR vibrational modes. In the attempt to fill these knowledge gaps, we applied far-IR spectroscopy to small, aromatic molecules of biological importance, which have a relatively low number of vibrational modes in the far-IR and are amenable to highly-accurate quantum-chemical calculations and detailed vibrational assignment. Isomer- and conformer-specific far-IR features of cold isolated aminophenol and methylacetanilide molecules were obtained with IR-UV ion-dip spectroscopy and assigned with the help of quantum chemical calculations. The observed far-IR transitions associated with deformation of the peptide link, an important structural unit in proteins, were found to be highly sensitive to the peptide link planarity, trans/cis configuration, and hydrogen bonding.

The powerful conformer-selective IR-UV ion-dip spectroscopy technique applied in the first part of the thesis is unfortunately restricted to molecules that possess an aromatic UV-absorption chromophore. The studies presented in the second part of the thesis attempt to circumvent this limitation by introducing a novel approach that combines cooling of molecules in a supersonic jet, IR multiple photon dissociation (IRMPD), vacuum ultraviolet (VUV) ionization, and mass spectrometry. The approach was

demonstrated by measuring the vibrational spectrum of the simplest peptide analog, N-methylacetamide, and its oligomers. The possibility to extract structural information from the IRMPD-VUV spectra was investigated for the Gly-Gly and Ala-Ala dipeptides, which are particularly interesting due to possible competition between their extended (β-strand like) and folded structures. The measured spectra for these dipeptides showed that the extended structure with weak hydrogen bonding interactions is strongly favored in the cold molecular beam due to its higher flexibility (larger entropy), as well as due to efficient collisional relaxation processes in the supersonic jet. The results show that even though IRMPD-VUV spectroscopy does not allow recording spectra of individual conformers, it nonetheless provides valuable structural information, especially for molecules that are not suited to conventional spectroscopy techniques.

Sammanfattning

Denna avhandling fokuserar på strukturanalys av isolerade molekyler av biologisk betydelse, med särskild betoning på utvecklingen av nya verktyg inom infraröd (IR) laserspektroskopi. I den första delen av avhandlingen undersöks tillämpningen av långvågig IR-spektroskopi (far-IR, $\lambda > 12$ μm) för strukturanalys genom att studera små aromatiska molekyler. Isomer- och konformer-specifika far-IR-signaturer hos kylda isolerade aminofenol- och metylacetanilidmolekyler bestämdes med IR-UV-dubbelresonansspektroskopi och identifierades med hjälp av kvantkemiska beräkningar. De observerade far-IR-övergångarna associerade med deformation av peptidlänken - en viktig strukturell enhet i proteiner - fanns vara mycket känsliga för planheten av peptidlänken, huruvida konfigurationen var trans eller cis, och de intilliggande intra- och intermolekylära vätebindningarna.

Denna kraftfulla konformer-selektiva metod, IR-UV-dubbelresonansspektroskopi, tillämpad i den första delen av avhandlingen är tyvärr begränsad till molekylerna som har en aromatisk UV-absorptionskromofor. De studier som presenteras i den andra delen av avhandlingen försöker kringgå denna begränsning genom att införa ett nytt tillvägagångssätt som kombinerar supersonisk strålkylning, IR-multifotondissociation (IRMPD), vakuum ultraviolett (VUV) jonisering och masspektrometri. Tillvägagångssättet demonstrerades genom att mäta vibrationsspektrumet för den enklaste peptidanalogen, N-metylacetamid, och dess oligomerer. Möjligheten att extrahera strukturell information från IRMPD-VUV-spektra undersöktes för Gly-Gly och Ala-Ala dipeptiderna, vilka är särskilt intressanta på grund av att de kan anta både utvidgade (β-strängliknande) och vikta strukturer. De uppmätta spektra för dessa dipeptider visade att den utvidgade strukturen med svaga vätebindningsinteraktioner är starkt föredragen i den kalla molekylära strålen på grund av dess högre flexibilitet (större entropi), såväl som effektiv kollisionsrelaxation i den supersoniska strålen. Resultaten visar att även om IRMPD-VUV-spektroskopin

inte kan producera ett spektrum från en enstaka konformer, ger det ändå värdefull strukturinformation, särskilt för de molekyler som konventionell spektroskopi inte passar för.

List of Papers

This thesis is based on the following research papers, which are referred to by their Roman numerals in the text.

I **Aminophenol isomers unraveled by conformer-specific far-IR action spectroscopy**
Vasyl Yatsyna, Daniël J. Bakker, Raimund Feifel, Anouk M. Rijs, and Vitali Zhaunerchyk
Phys. Chem. Chem. Phys., 2016, **18**, 6275-6283

II **Far-infrared Amide IV-VI spectroscopy of isolated 2- and 4-Methylacetanilide**
Vasyl Yatsyna, Daniël J. Bakker, Raimund Feifel, Anouk M. Rijs, and Vitali Zhaunerchyk
J. Chem. Phys., 2016, **145**, 104309

III **Infrared action spectroscopy of low-temperature neutral gas-phase molecules of arbitrary structure**
Vasyl Yatsyna, Daniël J. Bakker, Peter Salén, Raimund Feifel, Anouk M. Rijs, and Vitali Zhaunerchyk
Phys. Rev. Lett, 2016, **117**, 118101

IV **Conformational preferences of isolated glycylglycine (Gly-Gly) investigated with IRMPD-VUV action spectroscopy and advanced computational approaches**
Vasyl Yatsyna, Ranim Mallat, Tim Gorn, Michael Schmitt, Raimund Feifel, Anouk M. Rijs and Vitali Zhaunerchyk
Submitted for publication to *The Journal of Physical Chemistry*

V **Competition between folded and extended structures of alanylalanine (Ala-Ala) in a molecular beam**
Vasyl Yatsyna, Ranim Mallat, Tim Gorn, Michael Schmitt, Raimund Feifel, Anouk M. Rijs and Vitali Zhaunerchyk
In manuscript

Reprints were made with permission from the publishers.

Author's contribution to the papers

Paper I: Major part of experiment, data processing and quantum-chemical calculations; major part of writing

Paper II: Major part of experiment, data processing and quantum-chemical calculations; major part of writing

Paper III: Major part of experiment, data processing and quantum-chemical calculations; part of writing

Paper IV: Major part of experiment; part of data processing and quantum-chemical calculations; major part of writing

Paper V: Major part of experiment; part of data processing and quantum-chemical calculations; part of writing

Declaration

Some sections of this thesis were adapted from my licentiate ("half-way through PhD") thesis entitled "Far-infrared conformer-specific signatures of small aromatic molecules of biological importance", 2016.

Contents

List of Abbreviations

AP	**A**mino**P**henol
DFT	**D**ensity **F**unctional **T**heory
FEL	**F**ree **E**lectron **L**aser
FELIX	**F**ree **E**lectron **L**aser for **I**nfrared e**X**periments
FWHM	**F**ull **W**idth at **H**alf **M**aximum
HF	**H**artree-**F**ock
IR	**I**nfra**R**ed
IRMPD	**I**nfrared **M**ultiple **P**hoton **D**issociation
IVR	**I**ntramolecular **V**ibrational Relaxation
MA	**M**ethyl**A**cetanilide
MCP	**M**ulti**C**hannel **P**late detector
MD	**M**olecular **D**ynamics
NMA	**N**-**M**ethyl**A**cetamide
PES	**P**otential **E**nergy **S**urface
REMPI	**R**esonance **E**nhanced **M**ulti-**P**hoton **I**onization
TOF	**T**ime-**O**f-**F**light
THz	**T**era**H**er**z**
UV	**U**ltra**V**iolet
VPT2	Second-order **V**ibrational **P**erturbation **T**heory
VUV	**V**acuum **U**ltra**V**iolet

I dedicate this work to my family

Chapter 1

Introduction

1.1 Gas-phase spectroscopy for biomolecular structure elucidation

Every cell in our body consists of a large number and variety of biomolecules, such as proteins, nucleic acids and carbohydrates, that perform different tasks ranging from energy transfer and catalysis of chemical reactions to encoding information. The function and specific properties of a biomolecule is often closely related to its structure. For example, protein molecules perform a vast variety of functions in cells being polymers of twenty amino acids. They differ from one another in the amino acid sequence (called primary structure), which is encoded in DNA, and upon protein synthesis this sequence is translated into a three-dimensional shape that holds a certain function. The three-dimensional shape of a single polymer chain is referred to as a tertiary structure (see Fig. 1.1), whereas a protein complex, comprising several protein chains, is called a quaternary structure. Secondary structures (Fig. 1.1) correspond to local folded regions, such as α-helices and β-sheets, that are mostly stabilized by hydrogen bonding interactions. Our detailed understanding of how different proteins perform their function would probably not be possible without being able to zoom into their structure to the level of individual atoms. This, for example, can be done by means of X-ray diffraction crystallography [1], the technique which has already been used to determine more than one hundred thousands structures of proteins that can be crystallized.

An alternative method to study structure of biomolecules is to employ *spectroscopy*, which studies how the molecule interacts with electromagnetic radiation (light) as a function of its

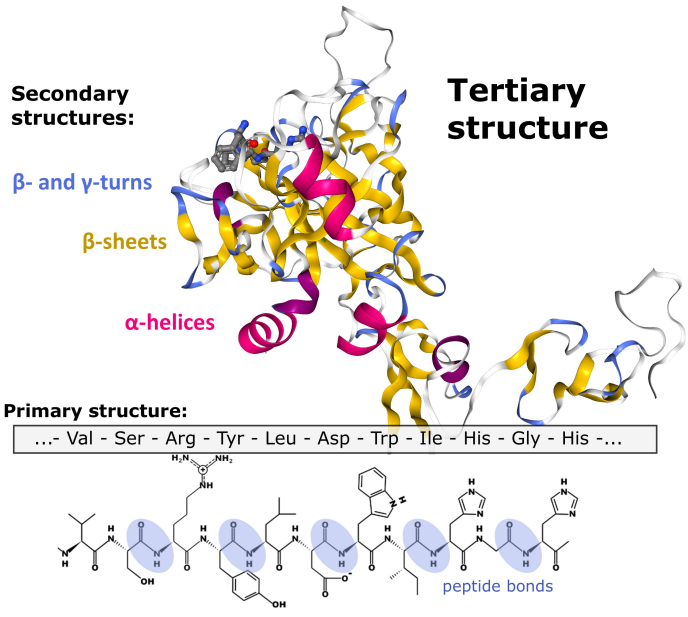

Figure 1.1: Different levels of structure in proteins: primary (amino acid sequence), secondary (local folding shapes such as α-helices) and tertiary (three-dimensional shape). The picture illustrates the structure of Human activated protein C (PDB ID: 1AUT), taken from RCSB PDB [2], depicted by NGL viewer [3] in "cartoon" representation.

wavelength (or frequency). For example, nuclear magnetic resonance (NMR) spectroscopy [4] uses radio waves to excite nuclei of molecular sample, placed in a strong magnetic field, and this method is used to study structure and dynamics of proteins in the solution, even those that cannot be crystallized. Rotational spectroscopy uses microwave radiation to probe the rotational transitions in molecules and is another tool to obtain structure of small biomolecular building blocks [5]. In this thesis, *infrared (IR) spectroscopy* is employed for structural analysis. IR spectroscopy studies how the IR light is absorbed by molecules due to excitation of different molecular vibrations, such as stretching, bending, and other deformations of molecular structural units. Only the so-called *IR-active* vibrations, which correspond to some changes in the molecular dipole moment, absorb IR light. Every molecular vibration has its own resonant frequency, the

value of which depends on different forces and the environment around the vibrating atoms. IR spectroscopy measures vibrational frequencies and absorption intensities, and is very sensitive not only to the strength of the covalent bonds that are elongated and contracted in the course of vibrations, but also to various intra- and inter-molecular forces that act upon each atom in a molecule. These include hydrogen bonding, dispersion and other non-covalent interactions [6] that are very crucial for stabilizing the three-dimensional structure of biomolecules.

Spectroscopy of *isolated* molecules aims to get information about intrinsic molecular properties, *i.e.* those which are not associated with the environment. For instance, the propensities of different amino acid sequences to form specific secondary structures in proteins can be studied by spectroscopy of isolated peptides [7–12]. Peptides are building blocks of proteins comprising short chains of amino acids connected by means of peptide bonds (Fig. 1.1). One of the methods to isolate molecules is to bring them into the *gas-phase*. Various techniques, applicable to biomolecules, exist for this purpose. It is worth mentioning electrospray ionization [13], matrix-assisted laser desorption/ionization [14], and laser-induced thermal desorption [7, 11, 15]. The latter technique is employed in this thesis for spectroscopy of isolated dipeptides. The common aspect of these techniques is that the molecules are transferred into the gas-phase in the low-pressure vacuum environment, and hence can be studied in nearly perfect isolation.

The interpretation of experimental IR spectra in the case of simple molecules can be based on previous empirical observations. For example, the typical IR peak positions related to the stretching of various molecular covalent bonds are well known. The same is true for the corresponding frequency shifts due to the formation of hydrogen bonds [9]. In the case of biomolecules, which can adopt many different three-dimensional structures, it is generally required to perform *quantum-chemical calculations*. These calculations aim to generate various stable three-dimensional structures that the studied molecule can adopt, and to calculate the vibrational spectra corresponding to each structure. By rotating the molecular structural units around single covalent bonds, molecular *conformations* can be generated. Such conformations do not always correspond to a stable molecular state, therefore a search of potential energy minima (geometry optimization) has to be performed. As a result, molecular *conformers* are found, which are the stable molecular conformations (see Fig. 1.2) that can

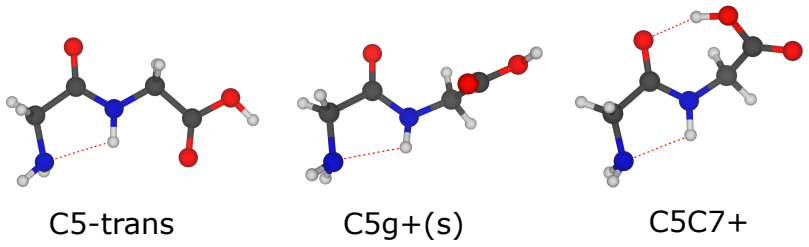

Figure 1.2: Several representative conformers of Gly-Gly dipeptide molecule, studied in this thesis. Hydrogen bonds are shown with dashed red lines. Carbon atoms correspond to grey, nitrogen - to blue, oxygen - to red, and hydrogen - to white.

potentially be present in the experiment. By comparing the calculated spectra of various conformers with the experimental spectra, we can conclude what conformers were present in the experiment, and evaluate the importance of different fundamental interactions that stabilize them.

Gas-phase IR spectroscopy offers several advantages in comparison with the condensed phase studies. The first advantage is that the gas-phase studies provide insight into intrinsic structural properties of molecules without influence of interactions with the surrounding solvent or crystalline environment. The second advantage is that the gas-phase experimental data can be directly compared to the quantum-chemical calculations, which are most easily applied to isolated molecules. Such direct comparison increases the reliability of the structural assignments, i.e. assignments of molecular structures responsible for the experimental spectra. Moreover, special gas-phase spectroscopic schemes, such as IR-UV double resonance technique [16, 17], offer a possibility to study each conformer, which the molecule adopts, individually. Thus, the experimental spectra can be used to "benchmark" and validate different theoretical approaches. As even the most advanced theoretical models involve certain approximations, such validation is very crucial and ensures further development in the field. The third advantage is that the conditions in the gas phase can be controlled to a large degree. For example, it is possible to study the bare molecule in a complex with only a few individual solvent molecules, which can be added to the isolated molecule one-by-one [8, 12]. Using this approach we can study how specific

intermolecular interactions affect the intrinsic structural preferences of biomolecules. As a final advantage, it is worth to mention that the gas-phase studies provide detailed understanding of the relationship between the IR spectra and the molecular structure, and this knowledge can be used to analyze spectra obtained in more complex (natural) environments.

1.2 Far-infrared gas-phase spectroscopy

IR photon energies within IR spectroscopy are commonly represented in wavenumbers, that is $1/\lambda$ in cm^{-1} units, where λ is the wavelength of radiation. The most widely-used photon energy range in the gas-phase IR spectroscopy, 3800–800 cm^{-1}, belongs to the so-called mid-IR region. Mid-IR spectroscopy mostly probes localized vibrations, which involve deformation of strong covalent bonds. For example, the vibrations associated with the stretching of the NH group of the peptide link, the so-called Amide A bands (3500–3250 cm^{-1}), are often probed when peptides are studied [9]. The Amide I and II bands (1450–1800 cm^{-1}), which correspond to C=O stretching and NH bending vibrations, respectively, are also very useful in peptide structure analysis. When NH and C=O groups of the peptide link take part in hydrogen bonding, the Amide I-II and Amide A bands are shifted in frequency. This makes mid-IR spectroscopy particularly useful for the studies of protein secondary structures, as they are largely stabilized by hydrogen bonds. On the other hand, spectroscopy of localized vibrations in the mid-IR range is not so suitable for distinguishing the structures with similar hydrogen bonding motifs but different three-dimensional shapes. This problem is particularly important in studies of larger molecules where many similar localized vibrations may give rise to congested spectral bands, from which only certain families of structures can be assigned [18–20]. In this respect, spectroscopy in the *far-IR range* ($<$800 cm^{-1}) can provide additional information [20]. It probes delocalized vibrations, as well as local vibrations with very shallow and anharmonic potentials. Such vibrations are sensitive to subtle variations in structure. The far-IR range also contains vibrations directly related to weak interactions important in biological molecules, such as hydrogen bonding and dispersion forces.

The unique features of far-IR spectroscopy make it highly suited for structural analysis of large and flexible biological molecules. Nevertheless, the routine application of far-IR spectroscopy

for structural analysis of isolated biomolecules is hindered by several obstacles. First, far-IR spectroscopy in the diluted gas-phase media requires a powerful light source, due to the fact that far-IR absorption cross-sections are typically low. And second, theoretical predictions of far-IR spectra are complicated by a high degree of anharmonicity and mode-coupling, thus impeding precise vibrational and structural assignment. Several sources of intense far-IR radiation are available nowadays, such as table-top single-pulse THz laser sources [21], synchrotron facilities [22], and free electron lasers [23]. Moreover, the availability of large-scale computing facilities, as well as powerful quantum-chemical models and molecular dynamics simulation approaches [20, 24–26] stimulates the development in the field. Still, the application of far-IR to structural analysis of large biological systems requires in-depth understanding of far-IR spectra of smaller biological building blocks. Thus, in the first part of this thesis we investigate the far-IR signatures of small, aromatic molecules of biological importance, which can be studied in a conformer-specific manner in the gas-phase, and are amenable to highly accurate quantum-chemical calculations and detailed vibrational band assignment.

1.3 Action spectroscopy techniques

Traditional IR spectroscopy measurements in the condensed phase are based on measuring the attenuation of IR light that passes through the optically dense sample. In the gas-phase, however, the low sample density restricts such measurements, and the so-called IR *action spectroscopy* techniques are usually applied [17, 27]. IR action spectroscopy detects the IR photon absorption by measuring a change in ionization or fragmentation yield, variation of fluorescence intensity, or electron detachment, for example. Within many action spectroscopy techniques, Infrared-Ultraviolet (IR-UV) double resonance spectroscopy [16, 17, 28] offers a remarkable advantage: it allows recording IR spectra of individual molecular conformers. This is achieved by probing the long-lived excited electronic states in molecules containing an aromatic UV-chromophore, using a tunable UV laser and employing Resonance Enhanced MultiPhoton Ionization (REMPI) in the case of neutral molecules [29], or UV photofragmentation in the case of ions [28]. The prerequisite for this technique is that the probed molecular ensemble is sufficiently cold (< 20 K), which implies that most of the molecules are found in their rovibrational *ground state*.

The IR laser excitation of the cold molecular ensemble changes the population of molecules being in the ground state, which effectively reduces REMPI or UV photofragmentation yield. This leads to observation of a dip in the ion signal, and therefore such technique is also called IR-UV ion-dip spectroscopy [17]. The IR-UV ion-dip spectroscopy is applied in the first part of this thesis to record conformer-specific spectra of small, aromatic molecules of biological importance, and is briefly described in Chapter 2.

1.4 IR spectroscopy of molecules without an aromatic UV-absorption chromophore

IR-UV double resonance spectroscopy provides a wealth of information about fundamental interactions responsible for molecular structure stabilization. This technique enables direct comparison of experimental spectra, measured for individual conformers, with theoretical calculations. The limitation of the IR-UV double-resonance spectroscopy is that it can only be applied to molecules with an aromatic UV-chromophore. In the context of peptide structural studies, it is worth to mention that among the twenty standard amino acids only three have an aromatic moiety in their R-group (Phe, Trp and Tyr). Carbohydrates, another example of an important class of biomolecules that do not have an aromatic chromophore, are also elusive to IR-UV spectroscopy technique. Chemical attachment of an aromatic chromophore [30–32] is most commonly applied to circumvent this issue, although such modification can change the intrinsic molecular properties by introducing extra non-covalent interactions, which may also alter the relative stabilities of molecular conformers [33, 34].

It is worth mentioning that when charged (ionized) biomolecules are investigated, several IR spectroscopy techniques, applicable to species without an aromatic moiety, are available. For example, tagging or “messenger” technique measures IR absorption by monitoring the abundance of weakly bound molecular clusters, which tend to fragment when exposed to resonant IR radiation [35]. Such weakly bound complexes can be sufficiently stable in the cold environment of the supersonic jet or a cold ion trap. The most widely-used tags are represented by rare gas atoms due to their low influence on the intrinsic properties of the tagged molecule. Another spectroscopy approach that is widely used in ion trap instruments is based on IR multiple-photon dissociation (IRMPD) [36], which is more generally applicable and

can also be used in the room temperature experiments. Both tagging and IRMPD spectroscopy techniques do not offer a possibility to record IR spectra of individual molecular conformers, but still provide a wealth of valuable information when charged molecules are investigated. IR spectroscopy of neutral isolated biomolecules that lack an aromatic ring remains challenging. Therefore, the second part of this thesis focuses on the development of a generally-applicable IR spectroscopy approach for structural analysis of neutral molecules. More specifically, we combine cooling in a supersonic-jet molecular beam, IRMPD spectroscopy, non-resonant VUV ionization and mass spectrometry to record IR spectra and perform structural analysis of peptides that are elusive to conventional IR spectroscopy techniques.

References

[1] J. C. KENDREW, G. BODO, H. M. DINTZIS, R. G. PARRISH, H. WYCKOFF, D. C. PHILLIPS, "A Three-Dimensional Model of the Myoglobin Molecule Obtained by X-Ray Analysis", *Nature* **1958**, *181*, 662.

[2] H. M. Berman, J. Westbrook, Z. Feng, G. Gilliland, T. N. Bhat, H. Weissig, I. N. Shindyalov, P. E. Bourne, "The Protein Data Bank", *Nucleic Acids Research* **2000**, *28*, 235–242.

[3] A. S. Rose, A. R. Bradley, Y. Valasatava, J. M. Duarte, A. Prlić, P. W. Rose, "NGL viewer: web-based molecular graphics for large complexes", *Bioinformatics* **2018**, *34*, 3755–3758.

[4] K. Wüthrich, "The way to NMR structures of proteins", *Nature Structural Biology* **2001**, *8*, 923.

[5] J. L. Alonso, J. C. López in *Gas-Phase IR Spectroscopy and Structure of Biological Molecules*, (Eds.: A. M. Rijs, J. Oomens), Springer International Publishing, Cham, **2015**, pp. 335–401.

[6] K. E. Riley, P. Hobza, "Noncovalent interactions in biochemistry", *Wiley Interdisciplinary Reviews: Computational Molecular Science* **2011**, *1*, 3–17.

[7] M. S. de Vries, P. Hobza, "Gas-Phase Spectroscopy of Biomolecular Building Blocks", *Annual Review of Physical Chemistry* **2007**, *58*, 585–612.

[8] K. Schwing, M. Gerhards, "Investigations on isolated peptides by combined IR/UV spectroscopy in a molecular beam – structure, aggregation, solvation and molecular recognition", *International Reviews in Physical Chemistry* **2016**, *35*, 569–677.

[9] W. Chin, F. Piuzzi, I. Dimicoli, M. Mons, "Probing the competition between secondary structures and local preferences in gas phase isolated peptide backbones", *Phys. Chem. Chem. Phys.* **2006**, *8*, 1033–1048.

[10] J. C. Dean, E. G. Buchanan, T. S. Zwier, "Mixed 14/16 Helices in the Gas Phase: Conformation-Specific Spectroscopy of Z-(Gly)n, n = 1, 3, 5", *J. Am. Chem. Soc.* **2012**, *134*, 17186–17201.

[11] *Gas-Phase IR Spectroscopy and Structure of Biological Molecules*, *Vol. 364*, (Eds.: A. M. Rijs, J. Oomens), Top. Curr. Chem., **2015**, 1–406, and references therein.

[12] N. S. Nagornova, T. R. Rizzo, O. V. Boyarkin, "Interplay of Intra- and Intermolecular H-Bonding in a Progressively Solvated Macrocyclic Peptide", *Science* **2012**, *336*, 320–323.

[13] J. Fenn, M Mann, C. Meng, S. Wong, C. Whitehouse, "Electrospray ionization for mass spectrometry of large biomolecules", *Science* **1989**, *246*, 64–71.

[14] M. Karas, D. Bachmann, U. Bahr, F. Hillenkamp, "Matrix-assisted ultraviolet laser desorption of non-volatile compounds", *International Journal of Mass Spectrometry and Ion Processes* **1987**, *78*, 53 –68.

[15] M. Handschuh, S. Nettesheim, R. Zenobi, "Is Infrared Laser-Induced Desorption a Thermal Process? The Case of Aniline", *The Journal of Physical Chemistry B* **1999**, *103*, 1719–1726.

[16] R. H. Page, Y. R. Shen, Y. T. Lee, "Local modes of benzene and benzene dimer, studied by infrared–ultraviolet double resonance in a supersonic beam", *The Journal of Chemical Physics* **1988**, *88*, 4621–4636.

[17] A. M. Rijs, J. Oomens in *Gas-Phase IR Spectroscopy and Structure of Biological Molecules*, (Eds.: A. M. Rijs, J. Oomens), Springer International Publishing, **2015**, pp. 1–42.

[18] A. M. Rijs, M. Kabelac, A. Abo-Riziq, P. Hobza, M. S. de Vries, "Isolated Gramicidin Peptides Probed by IR Spectroscopy", *ChemPhysChem* **2011**, *12*, 1816–1821.

[19] A. Rijs, N. Sändig, M. Blom, J. Oomens, J. Hannam, D. Leigh, F. Zerbetto, W. Buma, "Controlled Hydrogen-Bond Breaking in a Rotaxane by Discrete Solvation", *Angewandte Chemie International Edition* **2010**, *49*, 3896–3900.

[20] S. Jaeqx, J. Oomens, A. Cimas, M.-P. Gaigeot, A. M. Rijs, "Gas-Phase Peptide Structures Unraveled by Far-IR Spectroscopy: Combining IR-UV Ion-Dip Experiments with Born-Oppenheimer Molecular Dynamics Simulations", *Angewandte Chemie International Edition*, *53*, 3663–3666.

[21] C. Vicario, A. V. Ovchinnikov, S. I. Ashitkov, M. B. Agranat, V. E. Fortov, C. P. Hauri, "Generation of 0.9-mJ THz pulses in DSTMS pumped by a Cr:Mg2SiO4 laser", *Opt. Lett.* **2014**, *39*, 6632–6635.

[22] M. A. Martin-Drumel, O. Pirali, D. Balcon, P. Bréchignac, P. Roy, M. Vervloet, "High resolution far-infrared Fourier transform spectroscopy of radicals at the AILES beamline of SOLEIL synchrotron facility", *Review of Scientific Instruments* **2011**, *82*, 113106.

[23] D. Oepts, A. van der Meer, P. van Amersfoort, "The Free-Electron-Laser user facility FELIX", *Infrared Physics & Technology* **1995**, *36*, Proceedings of the Sixth International Conference on Infrared Physics, 297 –308.

[24] M.-P. Gaigeot, "Theoretical spectroscopy of floppy peptides at room temperature. A DFTMD perspective: gas and aqueous phase", *Phys. Chem. Chem. Phys.* **2010**, *12*, 3336–3359.

[25] V. Conti Nibali, M. Havenith, "New Insights into the Role of Water in Biological Function: Studying Solvated Biomolecules Using Terahertz Absorption Spectroscopy in Conjunction with Molecular Dynamics Simulations", *Journal of the American Chemical Society* **2014**, *136*, PMID: 25127002, 12800–12807.

[26] M. Thomas, M. Brehm, R. Fligg, P. Vohringer, B. Kirchner, "Computing vibrational spectra from ab initio molecular dynamics", *Phys. Chem. Chem. Phys.* **2013**, *15*, 6608 –6622.

[27] A. Cismesia, L. Bailey, M. Bell, L. F. Tesler, N. C. Polfer, "Making Mass Spectrometry See the Light: The Promises and Challenges of Cryogenic Infrared Ion Spectroscopy as a Bioanalytical Technique", *J. Am. Soc. Mass Spectrom.* **2016**, *27*, 757.

[28] N. S. Nagornova, T. R. Rizzo, O. V. Boyarkin, "Exploring the Mechanism of IR–UV Double-Resonance for Quantitative Spectroscopy of Protonated Polypeptides and Proteins", *Angewandte Chemie International Edition*, *52*, 6002–6005.

[29] Y. Shimozono, K. Yamada, S.-i. Ishiuchi, K. Tsukiyama, M. Fujii, "Revised conformational assignments and conformational evolution of tyrosine by laser desorption supersonic jet laser spectroscopy", *Phys. Chem. Chem. Phys.* **2013**, *15*, 5163–5175.

[30] I. Compagnon, J. Oomens, J. Bakker, G. Meijer, G. von Helden, "Vibrational spectroscopy of a non-aromatic amino acid-based model peptide: identification of the γ-turn motif of the peptide backbone", *Phys. Chem. Chem. Phys.* **2005**, *7*, 13–15.

[31] E. Gloaguen, M. Mons in *Gas-Phase IR Spectroscopy and Structure of Biological Molecules*, (Eds.: A. M. Rijs, J. Oomens), Springer International Publishing, Cham, **2015**, pp. 225–270.

[32] E. J. Cocinero, P. Çarçabal in *Gas-Phase IR Spectroscopy and Structure of Biological Molecules*, (Eds.: A. M. Rijs, J. Oomens), Springer International Publishing, Cham, **2015**, pp. 299–333.

[33] R. J. Plowright, E. Gloaguen, M. Mons, "Compact Folding of Isolated Four-Residue Neutral Peptide Chains: H-Bonding Patterns and Entropy Effects", *ChemPhysChem* **2012**, *12*, 1889–1899.

[34] E. Gloaguen, B. Tardivel, M. Mons, "Gas phase double-resonance IR/UV spectroscopy of an alanine dipeptide analogue using a non-covalently bound UV-tag: observation of a folded peptide conformation in the Ac-Ala-NH2–toluene complex", *Structural Chemistry* **2016**, *27*, 225–230.

[35] J. M. Lisy, "Infrared studies of ionic clusters: The influence of Yuan T. Lee", *The Journal of Chemical Physics* **2006**, *125*, 132302.

[36] J. Oomens, A. J. A. van Roij, G. Meijer, G. von Helden, "Gas-Phase Infrared Photodissociation Spectroscopy of Cationic Polyaromatic Hydrocarbons", *The Astrophysical Journal* **2000**, *542*, 404.

Chapter 2

Experimental Methods

In this chapter I will briefly describe the experimental techniques applied in this thesis. First, the supersonic-jet cooling method to achieve cold molecular beams will be explained. Second, different laser spectroscopy schemes will be presented. These include REMPI, IR-UV ion-dip and IRMPD-VUV action spectroscopy techniques. Finally, some details of the experimental implementation of these methods in a molecular beam setup will be presented.

2.1 Experiment: general remarks

In order to be able to elucidate structures of neutral (bio)molecules, an experimental apparatus has to satisfy several conditions. First, the studied molecules have to be isolated from any interactions that may affect their intrinsic structural properties. Nearly-perfect isolation of molecules at the time frame of the experiment can be achieved by transferring the molecules into the gas phase. Under this condition, the experimental observations can be directly compared with highly accurate quantum chemical calculations that are usually restricted to isolated molecules or molecular clusters. Second condition is that the molecular ensemble should have sufficiently low translational, rotational and vibrational temperatures (< 20 K). This requirement is demanded for high spectroscopic resolution as well as for the absence of hot bands which may otherwise hinder vibrational and structural assignments. Finally, the spectroscopic techniques that are applied to the biomolecular structure elucidation are required to provide sufficient structural information, especially when combined with quantum chemical calculations. For example, it should be possible to distinguish the isomers and conformers of the same molecule.

The first two conditions are fulfilled when a supersonic-jet molecular beam apparatus is used [1]. In such a setup the molecules are transferred to the gas-phase and introduced into a supersonic-jet expansion of a noble gas where they are cooled down. Afterwards, the produced cold gaseous molecules propagate to a high-vacuum interaction region where they are isolated from collisions or other interactions during laser irradiation time. Section 2.2 presents a brief description of the supersonic-jet cooling technique, while section 2.7 provides some details of the supersonic-jet molecular beam setup employed in this thesis.

The spectroscopic techniques that are applied in this thesis, namely REMPI spectroscopy, IR-UV ion-dip spectroscopy [1] and IRMPD-VUV spectroscopy [2], are described in sections 2.4, 2.5 and 2.6, respectively. These methods provide valuable information on the properties and structure of isolated molecules when combined with quantum-chemical calculations.

2.2 Supersonic-jet cooling

In order to allow for a precise structural characterization of gas-phase molecules based on their IR spectra, the spectra have to be free from features which may complicate vibrational assignment, such as hot bands and rotational broadening. Such complications are eliminated in supersonic-jet molecular beams, where the molecules are internally cooled through collisions with other species. As a result, the transitions from vibrationally excited states (hot bands) become negligible. Also, rotational contours of the vibrational transitions become substantially narrower than the bandwidth of an IR laser, which allows resolving most of the vibrational features in the measured IR spectra. Moreover, in cases where the molecule assumes several conformers in the gas phase, the supersonic-jet cooling enables measurements of conformer-specific IR spectra (see sections 2.4 and 2.5). Apart from cooling, the supersonic-jet expansion delivers isolated molecules into the laser interaction region, which is important for the studies of molecular properties that are not affected by perturbations coming from inter-molecular interactions. Alternatively, if the inter-molecular interactions are the key objects of study, the molecular associates (clusters) can be prepared and investigated.

A detailed description of the supersonic-jet cooling and its properties can be found in refs. [3–5]. Briefly, the reservoir with a monoatomic gas at a relatively high pressure P_0 is used, having a

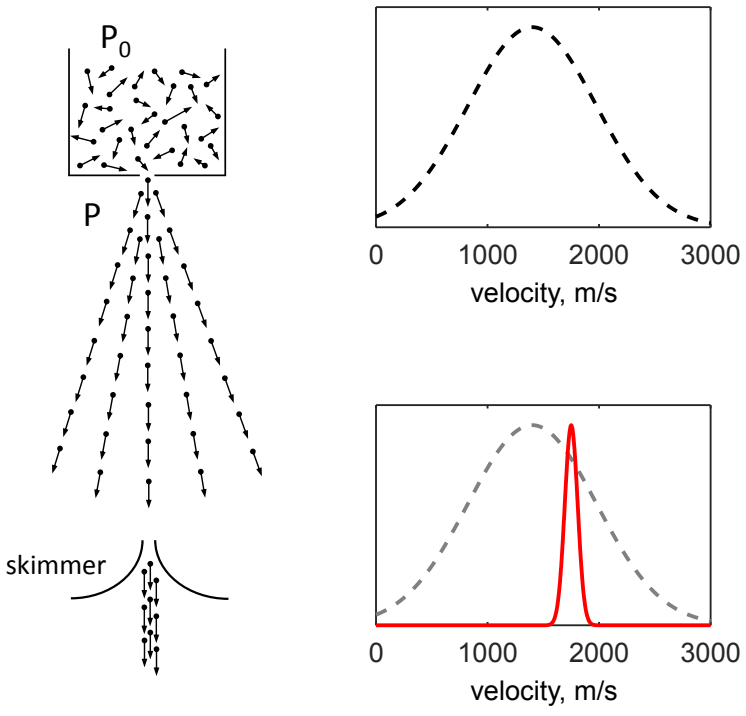

Figure 2.1: Schematic representation of a supersonic-jet molecular beam. Shown on the left is the expansion of the gas through the nozzle from the reservoir at high pressure P_0, into the vacuum chamber kept at much lower pressure P. The skimmer selects the coldest core part of the expansion. Shown on the right is the narrowing of the molecular velocity distribution due to selection of molecules with a large velocity component in the axial direction of the nozzle.

small orifice or shaped nozzle with diameter D. The gas from the reservoir penetrates through the nozzle into the vacuum chamber with background pressure P, much lower than P_0. If P_0 is high enough, the mean free path of the gas atoms is smaller than D, so only atoms having a large velocity component in the axial direction of the nozzle escape the reservoir (see Fig. 2.1). Due to subsequent multiple collisions, thermal motion is converted to directed translational motion with a flow velocity u that is higher than the local speed of sound. The ratio of u and the local speed of sound is called the Mach number, and as long as the Mach number is higher than one, the gas flow is called supersonic. It

can be seen from Fig. 2.1 that a drastic narrowing of the velocity distribution is achieved in a supersonic flow, *i.e.* most of the gas atoms are moving with the same speed. This implies a significant reduction of the translational temperature of the gas.

In order to achieve a supersonic molecular beam, a small fraction of molecules of interest is seeded into a large quantity of a carrier gas that undergoes supersonic flow. As the seeded molecules follow the directed supersonic-flow of the carrier gas, the velocity distribution of the seeded molecules becomes narrow too. Moreover, multiple collisions of the molecules with the carrier gas atoms result in the removal of internal energy stored in molecular vibrational and rotational degrees of freedom. Such cooling in seeded molecular beams is widely applied in high-resolution gas-phase spectroscopy studies. Seeding is done either by means of thermal evaporation in the case of volatile sample molecules, or by laser-induced thermal desorption [6–8] in the case of low-volatile and/or thermolabile molecules. Noble gases He, Ar or Xe at high pressure (2-10 bar) are typically used as carrier gases.

The operation of the supersonic jet requires substantial vacuum pumping in order to maintain sufficiently low background pressure in the vacuum chamber ($\leq 10^{-5}$ mbar). This is required to reduce the number of unwanted collisions of the expanding gas particles with the background gas, which can otherwise lead to a significant reduction of the flow velocity and Mach number. Instead of a continuous gas flow, pulsed expansion is used to achieve lower pressure in the vacuum chamber during the jet operation. Moreover, the flow of the gas can be collimated with a carefully-manufactured conical-shaped aperture (skimmer), which allows for differential pumping and selects the coldest part of the expansion region. This results in a narrow supersonic beam with high speed and narrow velocity distribution (see Fig. 2.1).

The temperature, pressure, density, and Mach number in the expansion region relate to each other according to thermodynamic laws, if desirable conditions for isentropic expansion are preserved (no viscous forces, shock waves, and heat sources or sinks such as chemical reactions etc.) [3]. For an ideal gas these relations are given by

$$T/T_0 = \left(\frac{P}{P_0}\right)^{(\gamma-1)/\gamma} = \left(\frac{\rho}{\rho_0}\right)^{\gamma-1} = \left(1 + \frac{(\gamma-1)}{2}M^2\right)^{-1}, \tag{2.1}$$

where T, P and ρ are the temperature, pressure and density in the isentropic part of the expansion, respectively, while T_0, P_0 and ρ_0 are the temperature, pressure and density in the gas reservoir, respectively; γ is the heat capacity ratio $C_p/C_v > 1$, and M is the Mach number which is defined as the ratio of the flow velocity u to the local speed of sound. As can be seen from Eq. 2.1, since $P_0 >> P$, the translational temperature of the gas in the expansion decreases.

For continuous gas flow at distances larger than a few nozzle diameters downstream the nozzle [3] the Mach number is given by:

$$M = A(x/D)^{\gamma-1}, \tag{2.2}$$

where x is the distance from the nozzle, and A is a constant which depends on γ. For monoatomic gases $A = 3.26$. As an example, according to Eq. 2.2 and Eq. 2.1, the Mach number of 44 and the temperature of 0.5 K are achieved at the distance of 50 nozzle diameters downstream.

Translational temperatures of less than 2 K are typically obtained in supersonic-jet molecular beams [3, 4]. At such temperatures the velocity distribution is very narrow which implies that the energy of the collisions in the gas will be low. Such low-energy collisions of the seeded molecules with the bath of carrier gas atoms can remove the internal energy stored in the molecules. This means that the molecular rotational and vibrational temperature can be equilibrated with the translational temperature of the supersonic flow. Rotational-translational equilibration is a rapid process in a supersonic-jet, and the rotational temperatures of 3-10 K are typically achieved [3, 5]. The vibrational-translation equilibration requires larger propagation distances from the nozzle where the density of the gas and hence the probability of collisions is lower. This implies that in many cases the vibrational temperature cannot reach equilibrium with the translational temperature. Thus, the vibrational cooling in a supersonic jet is less efficient and largely depends on the vibrational structure, but nevertheless results in a significant depopulation of the vibrationaly excited states. Under favorable conditions typical vibrational temperatures of 10-20 K are achieved.

2.3 Conformational relaxation in a supersonic jet

The conformational relaxation can lead to the phenomenon of "missing conformers", as evidenced in many jet-spectroscopy studies [9–14]. The relaxation process is dependent on many intrinsic factors such as internal energy, the number and type of bonds present, along with relaxation barriers and energy difference between isomers [9, 12, 15, 16]; and external factors such as temperature, and the energy transferred to the molecule via photons or collisions [15–21]. The relaxation barrier and energy difference between the conformers involved in the relaxation are among the most critical factors [9, 12, 15]. The studies of different small molecules with known energy barriers performed by Ruoff *et al.* [22] have shown that the relaxation is highly efficient if the barrier is lower than 400 cm^{-1}. However, studies of several amino-acids [9, 12] have shown that the critical barrier for the relaxation in an argon jet can be as high as 800 cm^{-1}. Aside from intrinsic determinants, the proportion of populated conformer species is also influenced by the type and polarizability of the carrier gas used in the jet-cooling setup [22]. The use of helium and neon as carrier gases would result in a larger number of populated conformers, while cooling with argon would decrease the number of observed conformers [9, 22].

2.4 REMPI spectroscopy

REMPI stands for Resonance Enhanced Multi-Photon Ionization, and the associated spectroscopic technique is schematically described in Fig. 2.2. The absorption of several photons is used to ionize the gas-phase molecules through an intermediate electronically excited state. The photons can either have the same or different wavelengths, which results in one-color or two-color REMPI schemes, respectively. REMPI spectroscopy is applicable to molecules that possess long-lived excited electronic states, such as Rydberg states in small molecules [23]. REMPI spectroscopy of medium-sized and large molecules is only possible when they possess an aromatic moiety, such as a phenyl ring [1]. It has a relatively long-lived electronically excited singlet-state (S_1) enabling the absorption of the second photon to ionize the molecule, and resulting in sharp absorption peaks. Moreover, the transitions from the electronic ground state (S_0) to the excited state

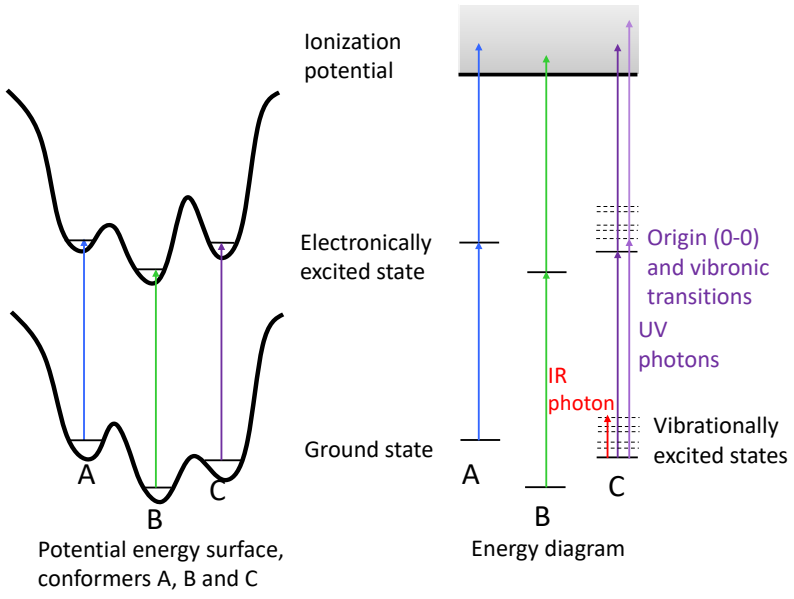

Figure 2.2: Schematic description of the one-color (1+1) REMPI spectroscopy technique. Shown on the left is a one-dimensional potential energy surface for the cooled molecules existing as three distinct conformers A, B, and C. REMPI spectroscopy probes the electronically excited states of the conformers, using the photon energies which slightly differ for the different conformers, thus allowing conformer-specific studies. In the (1+1) REMPI scheme two UV photons of the same energy are absorbed leading to the ionization of the molecular conformers.

(S_1) have a large oscillator strength for the phenyl ring, making REMPI spectroscopy an efficient and sensitive tool to study aromatic molecules.

REMPI spectra are typically recorded in the vicinity of the origin transition ($S_0 \rightarrow S_1$) with the help of a dye laser, producing frequency-tunable UV radiation. The origin transition is usually the strongest one in the REMPI spectrum and is denoted as "0-0" meaning that the electronic transition takes place between the states in their vibrationally ground states. Transitions with frequencies above the origin are vibronic transitions, implying that the molecule is electronically and vibrationally excited. REMPI spectra can also contain transitions with frequencies below the

origin, which are named hot bands. Hot bands appear when the molecular ensemble is not cold enough, such that some molecules are in a vibrationally excited electronic ground state. Despite the fact that hot bands complicate REMPI spectra, they can give some extra information. For example, the vibrational temperature of the molecular ensemble cooled in a supersonic-jet expansion can be estimated using the ratio between the integrated intensities of the hot band and the origin band [24].

REMPI spectroscopy is a very powerful method to distinguish between different conformers (rotational isomers) of the same molecule, that are populated in a molecular beam. Conformers have different molecular structures which results in different vibronic patterns observed with REMPI. Moreover, slightly different arrangement of the functional groups near a UV-chromophore leads to frequency shifts of the origin 0-0 transitions. As an illustration, Fig. 2.3 shows the REMPI spectrum of the 3-aminophenol molecule, studied in this thesis, which assumes two conformers denoted as *trans* and *cis*. As can be seen form Fig. 2.3, the origin transitions of the *trans* and *cis* conformers are observed at significantly different frequencies, which enables their selective excitation and ionization. Such selectivity of REMPI is employed in the IR-UV ion dip method, which allows measuring IR spectra

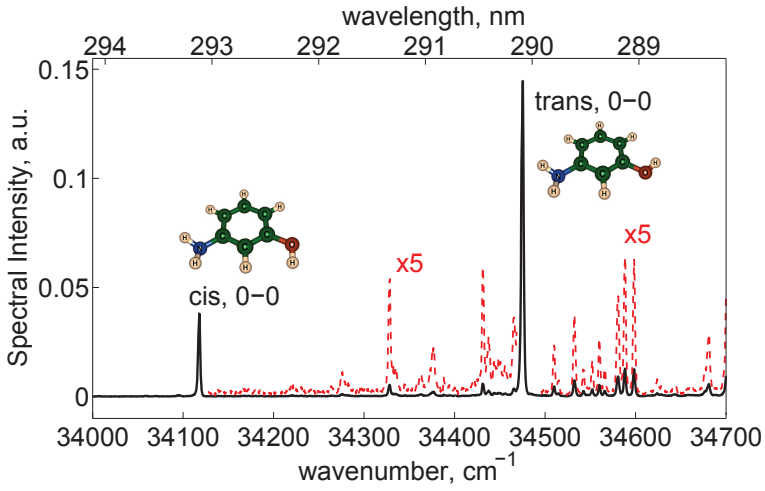

Figure 2.3: REMPI spectrum of 3-aminophenol. The origin transition peaks for the *trans* and *cis* conformers are denoted with "0-0".

of all molecular conformers, observed in the molecular beam, individually (see section 2.5).

With the help of two different tunable UV lasers one can also determine which peaks in the REMPI spectra are due to the same conformer. This is achieved by means of the UV-UV depletion and UV-UV hole-burning methods [6]. In these methods two tunable pulsed UV lasers subsequently interact with the molecules. The second laser pulse arrives shortly after the end of the first pulse. The laser which first interacts with the molecules is called the pump laser, and the second is called the probe laser. In the UV-UV depletion method the frequency of the probe laser is set to match the REMPI transition of one of the conformers, thus producing a constant ion signal. The frequency of the pump laser is scanned. When the frequency of the pump laser is resonant with the vibronic transition of the probed conformer, the population of its ground state is depleted, leading to a reduction of the ion signal produced by the probe laser. In this way the REMPI peaks coming from the same conformer will be identified. In the same manner UV-UV hole-burning spectroscopy is applied, with the only difference that the pump laser is fixed to the REMPI transition of one of the conformers, while the probe laser is scanned. In this case the REMPI spectrum is measured in which the peaks originating from the pumped conformer are removed.

The last aspect which should be noted here concerns the importance of cooling of the molecular ensemble. At room temperature the population of vibrationally and rotationally excited states becomes significant. This in turn leads to broad UV peaks that cannot be used to distinguish between different conformers. In contrast, high-resolution UV and IR spectra are obtained for a low-temperature molecular ensemble prepared with supersonic-jet cooling.

2.5 IR-UV ion-dip spectroscopy

IR-UV ion-dip spectroscopy is one of the key techniques in this thesis. It was first demonstrated by Lee and co-workers in 1988 [25]. It is also known as IR-UV double-resonance spectroscopy, as both IR and UV lasers are used to resonantly excite the molecule. It allows the measurements of conformer-specific IR spectra of cold gas-phase molecules cooled by supersonic-jet expansion. The principle of this method is illustrated in Fig. 2.4a. The frequency of the UV laser is tuned to match a REMPI transition of the specific

molecular conformer present in a molecular beam, thus creating a constant conformer-specific ion signal. Prior to the UV laser pulse, the molecular beam is irradiated with IR photons from a tunable IR laser. If the frequency of the IR laser is resonant with one of the vibrational transitions of the selected conformer, a fraction of molecules probed with the UV laser will be vibrationally excited leading to a reduction in the ion signal (see Fig. 2.4b). By scanning the IR laser frequency, IR-UV ion-dip spectra are recorded, showing all IR-active vibrational transitions of the selected conformer in the scanned frequency range. Individual IR-UV spectra of all conformers present in the molecular beam can be recorded in the same way by selecting their distinct REMPI transitions with a UV laser and scanning the IR laser frequency. The repetition rate of the UV laser is doubled with respect to the IR laser repetition rate, allowing IR on/off measurements to correct for the fluctuations in the molecular source output and long-term variations in the UV light power. In this case the relative absorption cross section $\sigma(\nu)$ can be obtained from the measured quantities using the following equation [26]:

$$\sigma(\nu) = \frac{1}{\Phi_{\mathrm{ph}}(\nu)} \ln\left(\frac{I_0}{I(\nu)}\right), \tag{2.3}$$

where I_0 is the ion intensity when the IR laser is off, $I(\nu)$ is the ion intensity when the IR laser is on, ν is the frequency of the IR laser and $\Phi_{\mathrm{ph}}(\nu)$ is the IR photon fluence.

It should be noted that the principle of the IR-UV ion-dip spectroscopy is very similar to that of the UV-UV depletion technique. As a measure of IR or UV photon absorption, the ion signal reduction is employed in both techniques. Its mechanism can however vary between the two techniques. The ion signal reduction in the UV-UV depletion technique originates from the pump laser efficiently depopulating the rovibrational state excited by the probe laser. This is also the case for the IR-UV ion-dip spectroscopy of small molecules with low density of vibrational states. For larger molecules, the vibrational excitation produced by the IR pump laser is rapidly redistributed to the background vibrational states. This results in IR "preheated" molecules that do not have "memory" about the initial vibrationally excited state pumped by the IR laser. Therefore, the ion signal reduction in this case originates from the difference between the UV absorption of the cold and IR "preheated" molecule; the latter typically shows broadening of the UV transitions [27, 28].

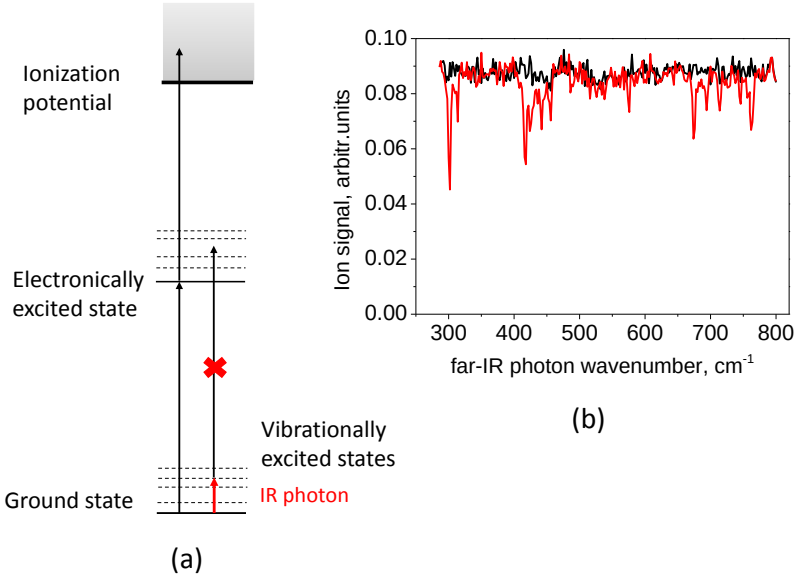

Figure 2.4: Schematic description of IR-UV ion-dip spectroscopy technique (a), and an experimental IR-UV ion-dip spectrum of *trans* 3-aminophenol (b), shown as illustration of characteristic wavelength-dependent ion-dip signals.

2.6 IRMPD-VUV action spectroscopy

2.6.1 Introduction

The main advantage of IR-UV ion-dip spectroscopy is the possibility to study conformers of the same molecule individually. This technique is however limited to small molecules, or those that have an aromatic UV chromophore, such as a phenyl ring. This limitation is particularly important in the studies of biomolecules such as peptides and carbohydrates. For example, only three out of twenty genetically encoded proteinogenic amino acids have an aromatic sidechain, which limits the scope of peptides that can be studied. Carbohydrate molecules do not have such a UV chromophore. One can use chemical attachment of an aromatic ring [29, 30], but this can be a difficult task, and moreover, such chemical modification might change the conformational space of the molecule of interest.

An alternative approach that does not require an aromatic chromophore was developed and implemented in this thesis. It is based on infrared multiple photon dissociation (IRMPD) spectroscopy combined with vacuum ultraviolet (VUV) photoionization. In the IRMPD process the resonant absorption of many IR photons leads to dissociation of the molecule, typically breaking the weakest molecular bond(s). Vibrational structure of the molecule can thus be studied by scanning the frequency of the IR laser and measuring the dissociation (fragmentation) yield at each frequency step. IRMPD spectroscopy has proven to be very successful in the studies of gas-phase ionized species stored in ion traps [31–33], due to its applicability to a broad range of molecules, that, for example, can be produced by electrospray ionization methods [34]. Moreover, trapped ions can be irradiated with IR laser light for a prolonged period of time which makes the IRMPD process highly efficient. In order to apply IRMPD spectroscopy to the studies of neutral species, a prolonged irradiation with the IR laser light has to be implemented as well, and, moreover, one has to be able to analyze the neutral dissociation products. For specific dissociation products, such as the OH radical generated with IRMPD of vibrationally pre-excited methanol [35], one can apply laser-induced fluorescence. A more general detection of both the precursor molecule and the dissociation products is required for implementation of IRMPD spectroscopy as an universal action spectroscopy tool. This aspect is fulfilled by using single-photon vacuum ultraviolet (VUV) laser photoionization and mass-spectrometry detection, applied in this thesis.

2.6.2 IRMPD process

The extended discussion of the IRMPD process and the overview of the literature on the topic can be found in ref. [1], while here a brief description will be presented. Fig. 2.5 shows a schematic representation of the IRMPD mechanism. If the frequency of the IR light matches the fundamental transition ($\nu_i = 0 \rightarrow 1$) of a certain (ith) vibrational mode, it can be excited. Direct subsequent excitation of the same mode with the IR photon of the same energy is not possible as the energy level spacing generally decreases with the increase of vibrational quantum number ν_i, due to anharmonicity of the molecular potential. Nevertheless, the anharmonic terms in the potential also lead to coupling between different vibrational modes, allowing dissipation of energy from

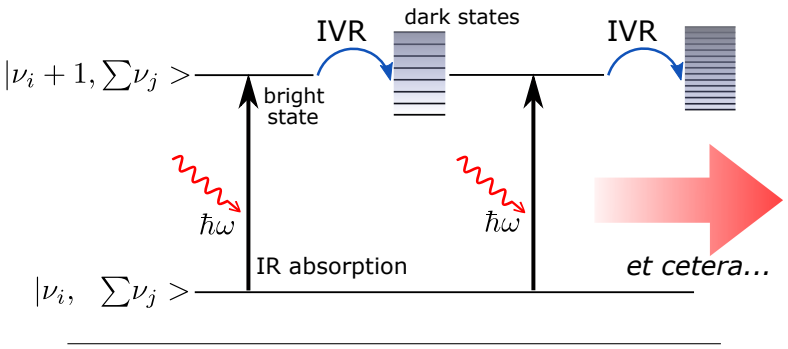

Figure 2.5: Schematic representation of the IRMPD mechanism.

one mode to another. This can lead to deactivation of the IR excited vibrational state. The available iso-energetic states for such energy deactivation typically correspond to combination modes. Once the deactivation of the fundamental vibrational state ν_i happens, another IR photon can be absorbed on the same fundamental transition. These processes can repeat many times gradually increasing the energy of the molecule until the molecule dissociates.

The above-mentioned deactivation of the excited vibrational level is known as intramolecular vibrational redistribution (IVR) [36], and the rate of this process determines the efficiency of the multiple photon excitation in IRMPD. In general, the efficiency of the IVR process depends both on the density of the vibrational states and on the average coupling strength between the states. Sufficiently high density of states ensures that the IR-laser excited vibrational mode (bright state) is coupled with a sufficient number of other states (dark states) such that the vibrational deactivation can occur. If this condition is satisfied, the IVR rate is mostly determined by the average coupling strength between the bright and dark states [37]. The long-established "tier" models of IVR [37–39] propose that the energy deposited by the IR laser into the vibrational excitation (bright state) is first transferred to a few states, called tier-1 states, which are strongly coupled to the bright state. From these tier-1 states the energy is further dissipated to a larger number of tier-2 states, and so on [37]. Theoretical studies show that for the fast energy dissipation there should be sufficiently strong coupling between the bright state and the dark tier-1 states [37–39]. These dark states should in turn be coupled to other states to avoid a bottleneck in the

energy flow. Thus, the average coupling strength between the states determines how quickly relaxation happens, while the high density of states ensures that vibrational excitation can go away from the bright state [1]. Experimental studies show that IVR lifetimes of medium-sized molecules can be as short as a fraction of a picosecond [37].

The anharmonicity that governs the multiple-photon excitation process in the IRMPD also has some effect on the appearance of the final spectra recorded with this technique. Slight *red-shifts* of the observed vibrational bands with respect to the one-photon spectra are expected, up to a few % of the center frequency. This effect originates from the excitation of many vibrational degrees of freedom following the IVR process, and these excitations in turn affect the frequency of the original transition, pumped with the IR laser, through anharmonic couplings. The red-shift is convoluted with the bandwidth of the laser up to the extent that the red-shifted vibrational band can go off-resonance with the narrow-band laser excitation, terminating the subsequent IR excitation. Nevertheless, the molecular excitation due to the absorption of the first few IR photons can result in a quasicontinuum of vibrational levels that can be incoherently excited by the IR laser [40]. Absorption of many IR photons in the quasicontinuum eventually result in unimolecular dissociation, leading to observable IRMPD signals. Another phenomenon that affects the IRMPD spectra is called *statistical inhomogeneous broadening* [41] of the vibrational bands. It originates from the fact that at a certain vibrational energy, deposited into the molecule through multiple photon excitation, various combinations of the excited vibrational modes and their occupation numbers are possible [41]. Each set of the excited vibrational modes in turn leads to a different red-shift of the main vibrational transition pumped by the IR laser. As IRMPD spectroscopy probes an ensemble of molecules that dissociate after reaching certain high vibrational excitation (dissociation energy), the IRMPD transitions appear broadened.

2.6.3 Description of IRMPD-VUV approach

The IRMPD-VUV approach aims to measure IR spectra of cold isolated neutral molecules for structural analysis. For this, a molecular beam of cold gas-phase molecules is prepared, and is allowed to interact with tunable, intense IR laser radiation. When the frequency of the IR laser is tuned in resonance with a

certain vibrational mode of the molecule studied, it can dissociate due to the IRMPD process as described in section 2.6.2. A VUV laser pulse, that irradiates the molecules directly at the end of the IR laser pulse, is used to ionize the neutral molecules and their IRMPD dissociation products (fragments), such that they can be detected and analyzed with a mass spectrometer. The VUV photon energy (10.5 eV) is enough to ionize most of the organic molecules and their fragments in a single-photon process, making IRMPD-VUV spectroscopy applicable to a broad range of molecules. Detection with a mass spectrometer yields relative intensities of the parent molecule and its fragments at each frequency step of the IR laser. These measured quantities are then used to plot IRMPD spectra with the help of the following relation:

$$I_{\mathrm{IRMPD}}(\nu) = \ln\left(\frac{I_0}{I(\nu)}\right) = \ln\left(\frac{I_{\mathrm{fragm}}(\nu) + I(\nu)}{I(\nu)}\right), \qquad (2.4)$$

where I_0 is the parent ion intensity when the IR laser is off, $I(\nu)$ is the parent ion intensity when the IR laser is on, ν is the frequency of the IR laser, and I_{fragm} is the summed intensity of all IRMPD fragments. The IRMPD intensities obtained are typically normalized to the actual IR laser power at each frequency step, though this procedure should be implemented with some caution due to the multiple photon nature of the IRMPD process [42]. In practice, such power correction is helpful when IRMPD spectra are compared to quantum-chemical frequency calculations [43].

2.7 Supersonic-jet molecular beam setup

The scheme of the molecular beam setup that was applied in this thesis is presented in Fig. 2.6. The setup comprises three vacuum chambers: the source chamber, the interaction chamber and the detection chamber. In the source chamber the sample molecules are transferred into the gas phase and are seeded into a pulsed supersonic-jet expansion of a noble gas. In the interaction chamber the cold molecular beam interacts with pulsed radiation of an IR laser and a (V)UV laser. In the detection chamber, which comprises a time-of-flight mass spectrometer, the molecular ions produced by (V)UV laser photoionization are detected and mass analyzed. In what follows, the key components and processes involved in the experimental apparatus will be described.

2.7.1 Transferring the sample into the gas phase and cooling

Nearly all the samples studied in this thesis are solids that have low vapor pressure at room temperature, which means that sublimation methods are required to transfer the sample molecules into the gas phase. The simplest method is thermal heating, and it was employed to sublimate the molecules studied in Papers [I], [II] and [III]. In the molecular beam apparatus, it was implemented as follows (see also Fig. 2.6). The noble gas (helium or argon at 3 bar) passed through a resistively heated sample oven, kept at a constant high temperature (up to 190° C) in the source chamber. After the oven, a heated pulsed valve (Parker general valve Series 9) with a nozzle orifice of 0.5 mm was placed. The valve opened at a repetition rate of 20 Hz, delivering the carrier gas together with the sample molecules into the source chamber. This produced a supersonic-jet expansion that drastically reduced the translational, rotational and vibrational temperature of the sample molecules, as described in section 2.2. The temperature of the valve was kept 5-10° C higher than that of the sample oven in order to avoid condensation of the sample molecules on the nozzle aperture. The operation of the jet increased the pressure in the vacuum chamber from $\sim 10^{-7}$ mbar to $1{\cdot}10^{-5}$ mbar, which is too high for the operation of the detector used in the mass spectrometer. A skimmer ($\varnothing$=1 mm), positioned 3 cm downstream the nozzle (see Fig. 2.6), allowed for differential pumping of the source and interaction chambers, leading to typical pressures in the latter being better than 10^{-7} mbar. The skimmer also selected the coldest part of the expansion, and formed a collimated molecular beam. In the interaction region, the molecular beam was crossed with IR and (V)UV laser beams between the repeller and extractor plates of the time-of-flight mass spectrometer, such that the ionized molecules could be mass analyzed. The molecules were isolated at the time frame of the IR and UV spectroscopy experiment, i.e. they essentially did not undergo any collisions being in a high-vacuum environment of the interaction chamber.

Sublimation by thermal heating is a simple approach but it is not applicable to biological molecules such as peptides. The reason is that such molecules undergo thermal decomposition at temperatures that are required for their sublimation [44]. The thermal decomposition can be avoided by using instant heating produced by a short laser pulse. At extremely high heating rates achievable with lasers ($10^8 - 10^{12}$ K$\cdot$ s^{-1}), the desorption process

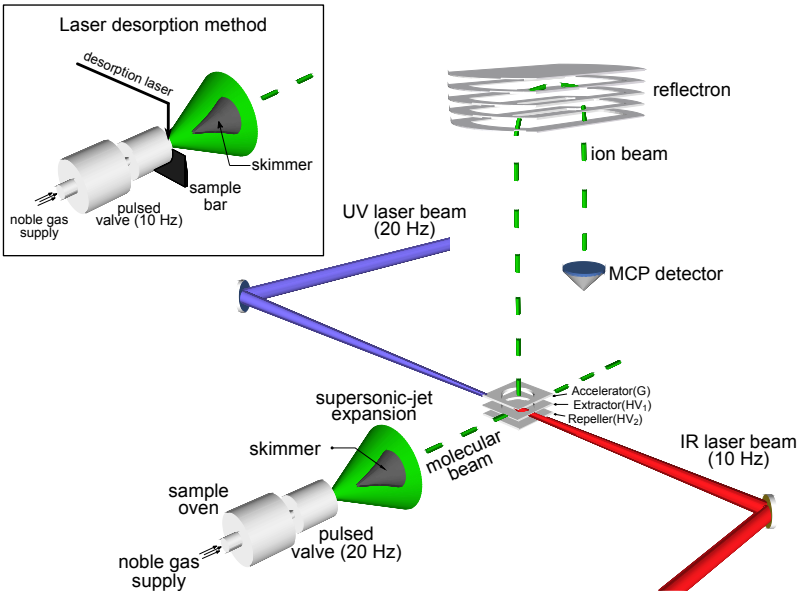

Figure 2.6: Scheme of the experimental setup for conformer-specific infrared spectroscopy of isolated molecules cooled in a supersonic-jet expansion.

of intact molecules is much more favorable then their decomposition [45, 46]. This effect is exploited in a laser-induced thermal desorption method [1] that was applied in our studies of neutral peptides presented in Papers [IV] and [V]. For this, the supersonic-jet molecular beam setup described above was slightly modified, see the inset in Fig. 2.6. A sample powder was mixed with carbon black in order to achieve a homogeneous grey-colored substance which was deposited on a graphite bar as a thin homogeneous layer. The sample bar was placed in front of a pulsed valve (0.5 mm nozzle orifice, Jordan TOF Products, Inc) in the source chamber. Pulsed radiation from the Nd:YAG laser ($\lambda = 1064$ nm, $1 - 2$ mJ/pulse) was gently focused on the sample bar surface and was used to desorb the sample molecules. During the experiment the sample bar was constantly moving with the help of the stepper motor in order to provide a fresh portion of the sample when the subsequent laser pulse arrives. The desorption plume was produced in front of the pulsed valve nozzle such that the desorbed molecules were captured by a supersonic-jet expansion

of argon. Here, the molecules were cooled down before entering the interaction chamber through the skimmer. For optimal cooling and molecular capturing conditions, the time differences between the argon gas pulse, the desorption laser and the (V)UV laser pulses were optimized using a standard delay generator (DG535, Stanford Research Systems).

2.7.2 (V)UV laser systems

The tunable UV laser radiation was produced by a dye laser from Radiant Dyes (Narrow Scan), pumped by the second (532 nm) or third harmonic (355 nm) of a Nd:YAG laser (Spectra Physics, Quanta-Ray Pro). The Nd:YAG laser delivered few-nanoseconds long pulses with pulse energy of around 200 mJ. The typical fundamental output of the dye laser in the visible range was 20 mJ/pulse. After frequency doubling, UV radiation pulse energies of around 2 mJ were achieved, with a pulse duration of a few nanoseconds. The tunable UV radiation of the dye laser was used for REMPI, as well as for selecting conformers in the IR-UV ion-dip spectroscopy scheme. In case the total energy of two UV photons was not exceeding the ionization energy of the studied molecule, a two-color REMPI(1+1') scheme was applied. The second color laser radiation with a wavelength of 193 nm was generated by an ArF excimer laser. The REMPI(1+1') scheme allowed selective excitation of molecular conformers using tunable UV radiation of the dye laser, followed by their subsequent ionization with the ArF laser radiation.

The VUV laser laser radiation with a wavelength of 118 nm ($h\nu$=10.5 eV) was produced by a third-harmonic generation process in a gas cell filled with Xe:Ar (1:10) gas mixture. At the front end of the gas cell, made of stainless steel, a quartz laser window was mounted. At the back end of the cell, a plano-convex MgF_2 lens with a radius of curvature of 56.6 mm was installed. The 118 nm radiation is strongly absorbed in air, therefore the gas cell was attached to the laser interaction vacuum chamber such that the back end of the cell was in vacuum. This enabled absorption-free propagation of the generated 118 nm light. To fulfill the third harmonic generation conditions, the pump laser radiation of the Nd:YAG laser with a wavelength of 355 nm (10 mJ/pulse) was focused in the center of the gas cell using a quartz plano-convex lens with a focal distance of $f = 35$ cm. The generated third-harmonic 118 nm laser beam was refocused into the molecular

interaction region through the MgF_2 lens. Due to the large refractive index difference of MgF_2 between the 118 nm and 355 nm beams, the residual 355 nm beam remained divergent and was not focused in the interaction region. Additional separation of the 118 nm and 355 nm beams in the molecular interaction region was accomplished using off-axis alignment through the MgF_2 lens. The estimated pulse energy of the generated VUV radiation is ≤ 0.5 μJ, based on the power conversion efficiency of 10^{-4} [47, 48] in phased-matched Xe-Ar mixture and the 50% transmission of the MgF_2 lens. This corresponds to $3 \cdot 10^{11}$ photons per pulse, and a peak power of 170 W. These values are low compared to the UV output of the dye laser ($\leq$ 2 mJ/pulse, $\leq$ 0.7 MW). However, the VUV laser output was used for single photon ionization which has lower intensity requirements compared to the two-photon ionization employed in UV dye laser experiments. Experimentally we have found that the VUV intensity was sufficient to obtain measurable signals of highly diluted molecular species, such as laser-desorbed peptides in a supersonic-jet molecular beam.

2.7.3 FELIX: tunable intense (far-)IR laser source

The IR spectra in this thesis were measured with the help of the IR free electron laser FELIX. A free electron laser (FEL) is a special type of lasers with unique features. FELs are characterized by high spectral brightness, narrow light bandwidth and essentially continuous wavelength tunability, which makes them highly suitable for many applications. The FELIX light source, for instance, allows accurate measurements of IR absorption spectra in extremely diluted (low-concentration) gas-phase environments, in a broad range of IR light frequencies.

In conventional lasers stimulated emission of radiation is obtained by creating a population inversion between higher and lower excited states of an active lasing medium. The emitted radiation with a frequency, equal to the difference between these two states, is amplified in a laser cavity, thus resulting in a coherent laser beam with a narrow bandwidth. To achieve tunability of the laser frequency, one can use optical parametric oscillators/amplifiers which are based on crystals with high quadratic optical nonlinearity. Certain laser media such as organic dyes also provide wavelength tunability, although the tuning range is limited to the choice of the media. In contrast, FELs do not have a strict limitation on the wavelength of the emitted radiation, as

the lasing medium in this case is represented by electrons traveling with relativistic speeds. The electrons propagate through a periodic magnetic field created by an array of magnets with alternating dipoles, called undulator, and perform a wiggling motion due to the Lorentz force, thus emitting radiation. The wavelength of the radiation is given by

$$\lambda = \frac{\lambda_u}{2\gamma^2}(1 + K^2), \tag{2.5}$$

where λ_u is the undulator period, K is a dimensionless parameter proportional to the strength of the magnetic field, and γ is the Lorentz factor

$$\gamma = \frac{1}{\sqrt{1 - \frac{v^2}{c^2}}}. \tag{2.6}$$

Here, v denotes the velocity of the electrons, and c is the speed of light. The K parameter is given by

$$K = \frac{eB\lambda_u}{2\pi m_e c}, \tag{2.7}$$

where e is the electron charge, B is the magnetic field strength and m_e is the electron rest mass. As can be seen from equations 2.5-2.7, the wavelength of the radiation can be tuned by changing the energy (velocity) of the electrons, and the strength of the magnetic field B. The latter can easily be tuned by changing the gap between the undulator magnets, whereas the undulator period λ_u is usually kept fixed.

The FEL principle allows achieving laser radiation in a very broad spectral range spanning from microwaves to X-rays. Of course, the electron energies required for the light generation in the X-ray domain are much higher than in the microwave region, therefore, FELs are typically designed to cover only a certain frequency range depending on their applications. The FELIX free electron laser facility, used in this thesis, is mainly applied for spectroscopy in the IR to THz region. The facility comprises several FELs, two of which, FEL-1 and FEL-2, cover the spectral range of 3-150 μm (3200-80 cm^{-1}). Several electron energies are used in this case to cover such a broad range. In this thesis, the typical frequency range used for gas-phase vibrational spectroscopy is 220-1850 cm^{-1}. It can be obtained by continuous scans from 220 to 800 cm^{-1}, and from 650 to 1850 cm^{-1}, by means of changing the undulator gap while the electron beam

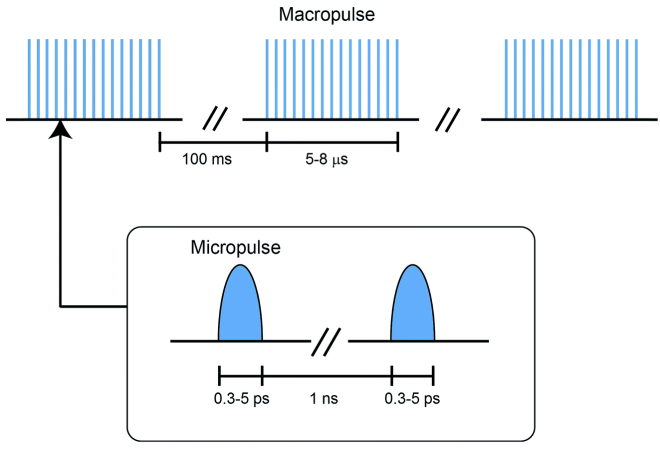

Figure 2.7: Pulse structure of radiation generated by the FELIX free electron laser. The figure is taken from Ref. [49], licensed under Creative Commons Attribution 3.0 Unported Licence. The original figure was not changed.

energy is kept fixed for each range.

The output laser radiation coming from FELIX consists of 5-8 μs long macropulses (see Fig. 2.7) with typical energies in the range of 50-100 mJ. Each macropulse consists of a train of bandwidth-limited micropulses with a duration of 0.3-5 ps. The bandwidth of the radiation can be optimized in the range of 0.5-5 % of the center frequency (FWHM), with typical values of 0.6-1.0 % applied in this thesis. The pulse structure of FELIX is particularly suitable for IRMPD experiments, as the micropulses are separated by 1 ns, which is typically longer than the molecular IVR rate.

2.7.4 Time-of-flight mass spectrometer

A reflectron time-of-flight (TOF) mass spectrometer [50] from Jordan TOF Products was used in this thesis. In combination with the employed laser systems and the molecular beam apparatus it allows recording IR and UV wavelength-dependent high resolution mass spectra. In brief, the neutral molecular beam species are UV-photoionized between two plates, called repeller and extractor (see Fig. 2.6). A positive high voltage is applied to the repeller plate ($\sim$3500 V), while the extractor plate is kept

$\sim$1000 V lower. The third plate, positioned above the extractor plate, is called accelerator and is grounded. Both extractor and accelerator plates have apertures that are covered by stainless steel grids with $\sim$90% transmission each. The positive ions are pushed towards the TOF tube by the electric field between the repeller and extractor plates, and are further accelerated between the extractor and accelerator plates. After that, the ions enter the field-free region of the TOF tube where they are dispersed according to their mass to charge ratio, m/z. On the way to the micro-channel plate (MCP) detector, ions are reflected using an ion mirror, called a reflectron, which consists of many charged plates producing a retarding potential. In this way, the ions pass a larger distance than the actual length of the TOF tube, leading to an increased mass resolution. Moreover, the reflectron compensates for the initial spread of the kinetic energy of the created ions, further increasing the mass resolution. The TOF tube used for the experiments described in this thesis allows measuring mass spectra with mass resolution, $m/\Delta m$, higher than 2000.

References

[1] A. M. Rijs, J. Oomens in *Gas-Phase IR Spectroscopy and Structure of Biological Molecules*, (Eds.: A. M. Rijs, J. Oomens), Springer International Publishing, **2015**, pp. 1–42.

[2] V. Yatsyna, D. Bakker, P. Salen, R. Feifel, A. Rijs, V. Zhaunerchyk, "Infrared action spectroscopy of low-temperature neutral gas-phase molecules of arbitrary structure", *Physical Review Letters* **2016**, *117*, 118101.

[3] D. H. Levy, "Laser Spectroscopy of Cold Gas-Phase Molecules", *Annual Review of Physical Chemistry* **1980**, *31*, 197–225.

[4] M. V. Johnston, "Supersonic jet expansions in analytical spectroscopy", *TrAC Trends in Analytical Chemistry* **1984**, *3*, 58–61.

[5] T. A. Miller, "Chemistry and Chemical Intermediates in Supersonic Free Jet Expansions", *Science* **1984**, *223*, 545–553, and refs. therein.

[6] M. S. de Vries, P. Hobza, "Gas-Phase Spectroscopy of Biomolecular Building Blocks", *Annu. Rev. Phys. Chem.* **2007**, *58*, 585.

[7] *Gas-Phase IR Spectroscopy and Structure of Biological Molecules*, *Vol. 364*, (Eds.: A. M. Rijs, J. Oomens), Top. Curr. Chem., **2015**, 1–406, and references therein.

[8] M. Handschuh, S. Nettesheim, R. Zenobi, "Is Infrared Laser-Induced Desorption a Thermal Process? The Case of Aniline", *The Journal of Physical Chemistry B* **1999**, *103*, 1719–1726.

[9] P. D. Godfrey, R. D. Brown, F. M. Rodgers, "The missing conformers of glycine and alanine: relaxation in seeded supersonic jets", *Journal of Molecular Structure* **1996**, *376*, 65 –81.

[10] R. M. Balabin, "Conformational Equilibrium in Glycine: Experimental Jet-Cooled Raman Spectrum", *The Journal of Physical Chemistry Letters* **2010**, *1*, 20–23.

[11] R. M. Balabin, "The identification of the two missing conformers of gas-phase alanine: a jet-cooled Raman spectroscopy study", *Phys. Chem. Chem. Phys.* **2010**, *12*, 5980–5982.

[12] P. D. Godfrey, R. D. Brown, "Proportions of Species Observed in Jet Spectroscopy-Vibrational Energy Effects: Histamine Tautomers and Conformers", *Journal of the American Chemical Society* **1998**, *120*, 10724–10732.

[13] H. Valdes, D. Reha, P. Hobza, "Structure of Isolated Tryptophyl-Glycine Dipeptide and Tryptophyl-Glycyl-Glycine Tripeptide: Ab Initio SCC-DFTB-D Molecular Dynamics Simulations and High-Level Correlated ab Initio Quantum Chemical Calculations", *The Journal of Physical Chemistry B* **2006**, *110*, 6385–6396.

[14] B. Yang, S. Liu, Z. Lin, "Computational study on single molecular spectroscopy of tyrosin-glycine, tryptophane-glycine and glycine-tryptophane", *Scientific Reports* **2017**, *7*, 15869.

[15] U. Erlekam, M. Frankowski, G. von Helden, G. Meijer, "Cold collisions catalyse conformational conversion", *Phys. Chem. Chem. Phys.* **2007**, *9*, 3786–3789.

[16] P. Felder, H. Günthard, "Conformational interconversions in supersonic jets: Matrix IR spectroscopy and model calculations", *Chemical Physics* **1982**, *71*, 9 –25.

[17] Q. Zhan, S. J. Wright, R. Zenobi, "Laser desorption substrate effects", *Journal of the American Society for Mass Spectrometry* **1997**, *8*, 525 –531.

[18] T. F. Miller III, D. C. Clary, A. J.H. M. Meijer, "Collision-induced conformational changes in glycine", *The Journal of Chemical Physics* **2005**, *122*, 244323.

[19] G. M. Florio, R. A. Christie, K. D. Jordan, T. S. Zwier, "Conformational Preferences of Jet-Cooled Melatonin: Probing trans- and cis-Amide Regions of the Potential Energy Surface", *Journal of the American Chemical Society* **2002**, *124*, 10236–10247.

[20] B. C. Dian, A. Longarte, T. S. Zwier, "Conformational Dynamics in a Dipeptide After Single-Mode Vibrational Excitation", *Science* **2002**, *296*, 2369–2373.

[21] S.-K. E. Cristina, S. J. P. in *Handbook of High-resolution Spectroscopy*, American Cancer Society, **2011**.

[22] R. S. Ruoff, T. D. Klots, T. Emilsson, H. S. Gutowsky, "Relaxation of conformers and isomers in seeded supersonic jets of inert gases", *The Journal of Chemical Physics* **1990**, *93*, 3142–3150.

[23] M. Ashfold, S. Langford, R. Morgan, A. Orr-Ewing, C. Western, C. Scheper, C. de Lange, "Resonance enhanced multiphoton ionization (REMPI) and REMPI-photoelectron spectroscopy of ammonia", *The European Physical Journal D - Atomic Molecular Optical and Plasma Physics* **1998**, *4*, 189–197.

[24] T. R. Rizzo, O. V. Boyarkin in *Gas-Phase IR Spectroscopy and Structure of Biological Molecules*, (Eds.: A. M. Rijs, J. Oomens), Springer International Publishing, Cham, **2015**, pp. 43–97.

[25] R. H. Page, Y. R. Shen, Y. T. Lee, "Local modes of benzene and benzene dimer, studied by infrared–ultraviolet double resonance in a supersonic beam", *The Journal of Chemical Physics* **1988**, *88*, 4621–4636.

[26] T. Ebata, T. Watanabe, N. Mikami, "Evidence for the Cyclic Form of Phenol Trimer: Vibrational Spectroscopy of the OH Stretching Vibrations of Jet-Cooled Phenol Dimer and Trimer", *The Journal of Physical Chemistry* **1995**, *99*, 5761–5764.

[27] N. S. Nagornova, T. R. Rizzo, O. V. Boyarkin, "Exploring the Mechanism of IR–UV Double-Resonance for Quantitative Spectroscopy of Protonated Polypeptides and Proteins", *Angewandte Chemie International Edition*, *52*, 6002–6005.

[28] M. Schmitt, F. Spiering, V. Zhaunerchyk, R. T. Jongma, S. Jaeqx, A. M. Rijs, W. J. van der Zande, "Far-infrared spectra of the tryptamine A conformer by IR-UV ion gain spectroscopy", *Phys. Chem. Chem. Phys.* **2016**, *18*, 32116–32124.

[29] I. Compagnon, J. Oomens, J. Bakker, G. Meijer, G. von Helden, "Vibrational spectroscopy of a non-aromatic amino acid-based model peptide: identification of the gamma-turn motif of the peptide backbone", *Phys. Chem. Chem. Phys.* **2005**, *7*, 13–15.

[30] E. J. Cocinero, P. Çarçabal in *Gas-Phase IR Spectroscopy and Structure of Biological Molecules*, (Eds.: A. M. Rijs, J. Oomens), Springer International Publishing, **2015**, pp. 299–333.

[31] J. R. Eyler, "Infrared multiple photon dissociation spectroscopy of ions in Penning traps", *Mass Spectrometry Reviews*, *28*, 448–467.

[32] N. C. Polfer, J. Oomens, "Vibrational spectroscopy of bare and solvated ionic complexes of biological relevance", *Mass Spectrometry Reviews*, *28*, 468–494.

[33] T. D. Fridgen, "Infrared consequence spectroscopy of gaseous protonated and metal ion cationized complexes", *Mass Spectrometry Reviews*, *28*, 586–607.

[34] J. Fenn, M Mann, C. Meng, S. Wong, C. Whitehouse, "Electrospray ionization for mass spectrometry of large biomolecules", *Science* **1989**, *246*, 64–71.

[35] O. V. Boyarkin, T. R. Rizzo, D. Rueda, M. Quack, G. Seyfang, "Nonlinear intensity dependence in the infrared multiphoton excitation and dissociation of methanol pre-excited to different energies", *The Journal of Chemical Physics* **2002**, *117*, 9793–9805.

[36] A. Chirokolava, D. S. Perry, O. V. Boyarkin, M. Schmid, T. R. Rizzo, "Intramolecular energy transfer in highly vibrationally excited methanol. IV. Spectroscopy and dynamics of 13CH3OH", *The Journal of Chemical Physics* **2000**, *113*, 10068–10072.

[37] K. K. Lehmann, G. Scoles, B. H. Pate, "Intramolecular Dynamics from Eigenstate-Resolved Infrared Spectra", *Annual Review of Physical Chemistry* **1994**, *45*, 241–274.

[38] A. A. Stuchebrukhov, R. A. Marcus, "Theoretical study of intramolecular vibrational relaxation of acetylenic CH vibration for v=1 and 2 in large polyatomic molecules (CX3)3YCCH, where X=H or D and Y=C or Si", *The Journal of Chemical Physics* **1993**, *98*, 6044–6061.

[39] A. A. Stuchebrukhov, A. Mehta, R. A. Marcus, "Vibrational superexchange mechanism of intramolecular vibrational relaxation in 3,3-dimethylbut-1-yne molecules", *The Journal of Physical Chemistry* **1993**, *97*, 12491–12499.

[40] N. Bloembergen, E. Yablonovitch in Laser Spectroscopy III, (Eds.: J. L. Hall, J. L. Carlsten), Springer Berlin Heidelberg, Berlin, Heidelberg, **1977**, pp. 86–93.

[41] A. A. Makarov, I. Y. Petrova, E. A. Ryabov, V. S. Letokhov, "Statistical Inhomogeneous Broadening of Infrared and Raman Transitions in Highly Vibrationally Excited XY6 Molecules", *The Journal of Physical Chemistry A* **1998**, *102*, 1438–1449.

[42] P. A. Schulz, A. S. Sudbo, E. R. Grant, Y. R. Shen, Y. T. Lee, "Multiphoton dissociation of SF6 by a molecular beam method", *The Journal of Chemical Physics* **1980**, *72*, 4985–4995.

[43] N. C. Polfer, "Infrared multiple photon dissociation spectroscopy of trapped ions", *Chem. Soc. Rev.* **2011**, *40*, 2211–2221.

[44] J. Schätti, U. Sezer, S. Pedalino, J. P. Cotter, M. Arndt, M. Mayor, V. Köhler, "Tailoring the volatility and stability of oligopeptides", *Journal of Mass Spectrometry*, *52*, 550–556.

[45] R. B. Hall, "Pulsed-laser-induced desorption studies of the kinetics of surface reactions", *The Journal of Physical Chemistry* **1987**, *91*, 1007–1015.

[46] R. R. Lucchese, J. C. Tully, "Laser induced thermal desorption from surfaces", *The Journal of Chemical Physics* **1984**, *81*, 6313–6319.

[47] A. H. Kung, "Third-harmonic generation in a pulsed supersonic jet of xenon", *Opt. Lett.* **1983**, *8*, 24–26.

[48] M. P. Lockyer, J. C. Vickerman, "Single Photon Ionisation Mass Spectrometry Using Laser-Generated Vacuum Ultraviolet Photons", *Laser Chemistry* **1997**, *17*, 139–159.

[49] D. Mani, T. Fischer, R. Schwan, A. Dey, B. Redlich, A. F. G. Van der Meer, G. Schwaab, M. Havenith, "A helium nanodroplet setup for mid and far-infrared spectroscopy using pulsed-free-electron lasers: vibrational spectra of propargyl alcohol", *RSC Adv.* **2017**, *7*, 54318–54325.

[50] B. A. Mamyrin, V. I. Karataev, D. V. Shmikk, V. A. Zagulin, "The mass-reflectron, a new nonmagnetic time-of-flight mass spectrometer with high resolution", *Zh. Eksp. Teor. Fiz.* **1973**, *64*, 82–89.

Chapter 3

Computational Methods

In this chapter, I will briefly describe the computational methods applied in this thesis. The aim of the calculations is to interpret the measured vibrational spectra of the studied molecules. The methods include conformational search, structure and energy calculations using quantum-chemical methods such as DFT, as well as harmonic and anharmonic frequency calculations.

3.1 Introduction

3.1.1 Wavefunction based methods

In quantum chemistry the principles of quantum mechanics are used for the description of different physical and chemical properties of molecules. If theoretical principles are solely used in calculations, with no empirical parameters or experimental data fitting, such quantum-chemical methods are called *ab initio*. Most of the quantum chemical methods rely on the solution of the Schrödinger equation with a Hamiltonian that describes the electrons and nuclei of the molecule. Such methods are called *wavefunction based* methods [1]. Certain approximations have to be applied, as the exact solution of the Schrödinger equation is not possible for systems larger than the hydrogen atom. The most important is the Born-Oppenheimer approximation [2], which decouples the movement of the atomic nuclei from the movement of electrons. It enables the separation of electron and nuclei coordinates, and allows solving the Schrödinger equation in two steps: first for electronic wavefunction, and then for the nuclear wavefunction. The electron wavefunction solutions and the associated electronic energies obtained at different fixed positions of the nuclei yield a potential energy surface (PES) that governs

the motion of the nuclei. The minima in the PES correspond to equilibrium molecular structures, and they can be found using molecular geometry optimization methods. Moreover, using the second-order energy derivatives in the vicinity of the PES minima one can obtain harmonic vibrational frequencies associated with the equilibrium structures.

The well-known Hartree-Fock (HF) approximation assumes that each electron only feels the Coulomb repulsion due to the average positions of all other electrons. The HF method typically allows accounting for 99% of the total electronic energy [1]. The remaining energy due to instantaneous interactions between the electrons is called correlation energy. The correlated methods, sometimes called post-HF methods, aim to describe this correlation energy to a various degree of detail, and provide a better accuracy of the calculated molecular properties with respect to the experiment.

In addition to the approximations discussed above, the calculations for many-electron systems have to rely on approximate electronic wavefunction. It can be constructed as a trial function with parameters that are typically optimized using the variational principle [1]. Slater determinant constructed from one-electron molecular orbital functions satisfies the Pauli principle, and is therefore used in the HF method. Each unknown one-electron molecular orbital function is in turn represented as a linear combination of known functions, such as Slater type [3] or Gaussian type [4] orbitals. The set of functions that are used for such representation is called *a basis set*. By using an infinite amount of basis set functions, which is known as a complete basis set, the unknown molecular orbital wavefunction can be described exactly. Of course this is not achievable in real calculations, and basis sets with a limited number of basis functions are used. The quality of the basis set, *i.e.* the accuracy of the description of the molecular orbitals, both depends on the number of functions used, and on how well a single basis set function can reproduce the orbital. The quality of the basis set also affects the general accuracy of the calculations, but owing to a steep scaling of the computational cost with the number of basis set functions, it should be reduced as much as possible without compromising the reliability of the results. One of the strategies to achieve this is to use a contracted basis set. In such a basis set the atomic core orbitals are partially described by a linear combination of known functions with fixed coefficients, while the valence region orbitals are fully optimized

using the variational principle. This approach generally provides reliable results as most of the chemistry in molecules is mainly determined by the valence electrons.

3.1.2 Density functional theory

In contrast to the wave-function based methods, *density functional theory* (DFT) relies on the principle that the ground state electronic energy is completely determined by the electron density function [5], reducing the complexity of the system with N electrons from 3N to 3 variables. The electronic energy of the system is approximated by means of a functional, *i.e.* function of a function, which relates the electron density $\rho(\vec{r})$, which is a function of Cartesian coordinates, to the energy. The energy functional $E[\rho]$ may be divided into three parts [1]:

$$E[\rho] = T[\rho] + E_{ne}[\rho] + E_{ee}[\rho], \tag{3.1}$$

where $T[\rho]$ is the kinetic energy term, $E_{ne}[\rho]$ corresponds to the attraction between nuclei and electrons, and $E_{ee}[\rho]$ corresponds to the electron-electron repulsion. By knowing the exact functional $E[\rho]$, one can obtain an exact result, which is equivalent to the full solution of the many-body Schrödinger equation in the wave-function based methods [6]. Finding the exact functional for all except the simplest systems is practically impossible [6], therefore approximate functionals are used. Nevertheless, many of the modern approximate functionals provide reliable accuracy for a broad range of problems in quantum chemistry. The major advantage of DFT methods is a favorable scaling of the computational cost versus the number of atoms (electrons), allowing accurate calculations for large systems at relatively low computational cost.

It should be noted that the most successful and widely-used implementation of DFT was proposed by Kohn and Sham [6, 7] (known as Kohn-Sham DFT), who re-introduced the orbitals into the initial orbital-free formulation of DFT. Kohn and Sham noted that the main flaw of the orbital-free DFT approach was the poor description of the kinetic energy, and they proposed to split it into two parts. The first part can be calculated exactly in a similar manner as in the HF method, where the Slater determinant is constructed and the orbital (basis set) coefficients are optimized to minimize the energy. The second, smaller part, is an exchange-correlation term that is approximated by means of a functional of

electron density ρ. The energy of the molecular system E_{DFT} can be then expressed as:

$$E_{\mathrm{DFT}}[\rho] = T_s[\rho] + E_{ne}[\rho] + J[\rho] + E_{xc}[\rho], \tag{3.2}$$

where $T_s[\rho]$ is the kinetic energy calculated using the Slater determinant, $E_{ne}[\rho]$ is the energy of attraction between nuclei and electrons, $J[\rho]$ is the Coulomb term of the electron-electron repulsion energy, and $E_{xc}[\rho]$ is the remaining exchange-correlation energy term. The widely-used Kohn-Sham DFT methods only vary by the choice of the functional that describes the last term, the exchange-correlation, which typically has a quite small contribution to the total energy but nevertheless is very important to describe molecular properties accurately. In practice, the selection of the DFT functional is based on its performance for the problem to which DFT is applied. Kohn-Sham DFT is the main quantum-chemical method applied in this thesis.

3.1.3 Treatment of vibrational anharmonicity

In the literature, the assignments of experimental IR spectra are typically based on quantum chemical calculations (*e.g.* DFT) where geometry optimizations and subsequent vibrational analysis in the *double harmonic approximation* are performed. The major goals of these calculations are to identify structures contributing to the experimental spectra and to reveal detailed information on the interactions that shape these structures. Within the double harmonic approximation the potential energy surface and dipole moment are truncated at the second and first order respectively, usually leading to overestimated vibrational frequencies and less accurate intensities. To overcome this drawback, different scaling methods for harmonic frequencies (or force fields) have been proposed [8–12], and are widely used to correct the band positions of the fundamental transitions. However, this approach is not always reliable, and is especially not suitable for the low frequency region due to significant anhramonic mode-coupling effects. Furthermore, harmonic frequency scaling does not give any information on the intensities of overtones and combination bands, which might be important for a correct analysis of experimental IR signatures.

There are several generally applicable methods which go beyond the harmonic approximation, and they can be divided into

dynamical (time-dependent) approaches, such as *ab initio* molecular dynamics (MD) simulations [13–15], and time independent approaches, with most effective implementations built on the second order-vibrational perturbation theory (VPT2) [16–18], and the vibrational self-consistent field (VSCF) approach [19]. *Ab initio* MD simulations are based on a classical treatment of the nuclei, and a quantum mechanical treatment of the electrons *e.g.* with DFT formalism [14]. The dynamics simulations are performed at finite temperatures and therefore they naturally describe conformational dynamics, as well as all anharmonic effects due to sampling of all accessible parts of the potential energy surface. Despite the high computational cost, this approach is particularly appealing when available experimental spectra are obtained at room temperatures, and hence contain natural broadening of the lines taking into account all populated conformations. It was also shown to be very successful in describing gas-phase far-IR spectra of peptide systems with a large number of torsional degrees of freedom [20–22].

Time independent VSCF computations are based on the approximation that each vibrational mode is moving in the mean field of the remaining vibrational motions. The total wave function of the VSCF approximation is a product of single mode wave functions, which are determined self-consistently. Despite a problematic description of strongly coupled vibrational modes and higher excited states due to correlation effects between the different modes, the VSCF approach was successfully applied to large systems of biological interest [19]. Correlation corrected modifications of the VSCF method (such as VSCF-PT2) increase the accuracy of the calculated vibrational transitions, but are limited to medium sized molecular systems with 20-30 atoms [23], due to an increased computational cost.

In this thesis the treatment of anharmonicity of vibrations in mid-IR and far-IR ranges is based on the vibrational second-order perturbation (VPT2) theory [16–18]. Within the VPT2 method, the 3rd and 4th order derivatives of the potential are calculated and treated as perturbations to the harmonic potential, and this problem is solved using the second-order perturbation theory. The VPT2 method was shown as a reliable tool for the prediction of fundamental vibrational transitions, as well as first overtones and combinational bands. It is considered to be especially effective for semi-rigid, isolated molecular systems [18], and most of the molecules studied in this thesis can be considered as such. It

should be noted, however, that the evaluation of the VPT2 approach carried so far [18] focused on the mid-IR region, while the far-IR vibrations were not always included due to the lack of experimental data. In this thesis such evaluations have been performed, as our far-IR experimental spectra were obtained under isolated gas-phase conditions and for individual molecular conformers. These two factors allow direct comparison with the results of *ab initio* calculations that are typically performed for isolated molecules in a single conformer.

3.2 Conformational search

Conformations are structures that can be inter-converted between each other using rotations about formally single bonds [24]. The aim of the conformational search is to generate all possible structures that a molecule can have under experimental conditions. When applied to the gas-phase studies of neutral organic molecules, this typically implies finding *conformers*, i.e. conformations which correspond to local minima on the potential energy surface.

A random search method [1, 25] was applied to generate conformers for the molecules studied in this thesis. In this method, an initial trial molecular structure is subjected to random changes in the dihedral angles associated with rotatable bonds. The generated random structure is then submitted to a geometry optimization algorithm with one of the available computationally inexpensive methods, such as force-field or semi-empirical methods. The optimized geometry is added to the list of the identified structures, and ranked according to its electronic energy. Duplicate structures generated are discarded based on their relative energies and structural similarity. A large amount of structures is generated in this way, typically until all the lowest-energy conformers up to a certain energy cut-off value were found more than 10-20 times. This indicates that the conformational search covered most of the available conformational space, in other words it is nearly exhaustive.

The generation of random conformers, their energy ranking and removal of duplicates was performed using a program written in C# [26], interfaced with MOPAC [27]. MOPAC, which stands for Molecular Orbital PACkage, is a quantum-chemistry program that enables energy calculations and geometry optimizations with semi-empirical methods. In particular, the PM6 (Parametrization

Table 3.1: List of typical DFT functionals applied in this thesis

Functional	Type[a]	Empirical Dispersion[b]	Reference
B97d	GGA	D2	[32]
B3LYP	Global hybrid-GGA	-	[31]
B3LYP-D3	Global hybrid-GGA	D3	[33, 34]
PBE0	Global-hybrid GGA	-	[35]
B97-1	Global-hybrid GGA	-	[36]
B3PW91	Global-hybrid GGA	-	[31]
M06-2X	Global-hybrid meta-GGA	-	[37]
ωB97X-D	Range-separated-hybrid GGA	D2 with damping	[38]

[a] GGA refers to generalized gradient approximation [39], global-hybrid GGA implies mixing local exchange approximation with non-local Hartree-Fock exchange [40]

[b] D2 and D3 refer to dispersion models by Grimme [32, 33]

Model 6) method, which employes NDDO formalism (neglect of diatomic differential overlap), and uses corrections for hydrogen bonding and dispersion interactions (PM6-D3H4 [28]) was mainly applied in our studies.

3.3 Accurate molecular structure and energy calculations

The accuracy of structure and energy calculations performed with semi-empirical methods such as PM6-D3H4 is not sufficient for comparison with experimental results. Therefore, the conformers identified in the conformational search were submitted for geometry optimization [29] and frequency calculations based on more accurate methods, such DFT and MP2, using the quantum-chemistry package Gaussian [30]. The selection of methods was based on their performance for similar molecular systems studied previously. Table 3.1 shows a representative list of DFT functionals applied in this thesis. All the listed functionals employ generalized gradient approximation (GGA), which basically implies that, in addition to the electron density, its first derivative is also included as a variable. Most of the applied functionals also mix local exchange energy (DFT) with non-local HF exchange, which typically improves the accuracy of the calculations. Such functionals are called hybrid. The hybrid B3LYP functional [31], widely-used for harmonic frequency calculations in molecules, uses 20% of HF exchange.

One of the drawbacks of DFT is that it does not account for dispersion forces [41, 42] that originate from interactions between instantaneous dipoles that appear in the molecular systems due to electron correlation effects. Several approaches to circumvent this problem exist [43]. The approach that relies on the addition of damped dispersion terms to the DFT energy (DFT-D) [32–34] is probably the most common in the literature. Alternatively, the DFT functional can be parametrized such that it can describe dispersion interactions, as in the case of the M06-2X functional [37].

The so-called composite methods, such as CBS-QB3 [44] and G4MP2 [45], can be used to achieve highly accurate relative energies of the conformers that were found in the conformational search. In these methods the energy of the structure optimized with DFT methods is calculated using a combination of several calculations, such as CCST(T), MP2 and HF with basis sets of different quality. The CBS-QB3 method attempts to reach the complete basis set limit in order to eliminate errors associated with the limited size of the basis sets.

3.4 Frequency calculations and VPT2 approach

3.4.1 Double harmonic approximation

In order to get valuable information on the molecular structure from experimental IR spectra, they have to be compared with theoretical spectra of the lowest-energy conformers found with the conformational search. As mentioned in section 3.3, every conformer is submitted to a geometry optimization algorithm [29] that adjusts the geometry until a local energy minimum of the molecular PES is found. The next step is to calculate the vibrational frequencies and intensities for the molecular structures obtained, which is usually done within the double harmonic approximation. For a harmonic oscillator the potential energy is described by a parabola $V = \frac{1}{2}kx^2$, where x is the displacement from the equilibrium position and k is the force constant. For a molecule with N atoms we can represent the potential energy by a Taylor expansion, which within the harmonic approximation is

truncated to a second order:

$$V(x_1, x_2, x_3, ...x_{3N}) = V_0 + \sum_{i=1}^{3N} \left(\frac{\partial V}{\partial x_i}\right)_{x_i=0} x_i + \\ + \frac{1}{2} \sum_{i,j=1}^{3N} \left(\frac{\partial^2 V}{\partial x_i \partial x_j}\right)_{x_i=x_j=0} x_i x_j \ + \ldots,$$

where V_0 is a constant, the second term is zero due to the optimized geometry (potential energy minimum), and the third term gives the force constants

$$k_{ij} = \left(\frac{\partial^2 V}{\partial x_i \partial x_j}\right)_{x_i=x_j=0} .$$

The force constant matrix (Hessian, $3N \times 3N$) is formed using the second-order partial derivatives of the potential. In the subsequent steps the force constants are represented using mass-weighted Cartesian coordinates $q_i = \sqrt{m_i} x_i$, and the Hessian is diagonalized yielding $3N$ eigenvectors and $3N$ eigenvalues. The square roots of the eigenvalues are the fundamental frequencies of the molecule. Six of them are nearly equal to zero and corresponds to three translational and three rotational modes. The remaining $3N - 6$ eigenvectors are normal modes, and have the meaning of independent fundamental vibrational motions, for which the center of mass does not move.

In the same manner the dipole moment can be represented by a Taylor expansion, though in this case it is truncated to first order. The first order derivatives of the dipole moment allow calculating harmonic intensities of the fundamental transitions for each normal mode.

3.4.2 Second-order vibrational perturbation theory (VPT2)

The VPT2 approach goes beyond the double harmonic approximation, and takes into account third- and forth-order derivatives of the potential, and second-order derivatives of the dipole moment [18]. The higher-order derivatives are calculated numerically, which requires evaluation of the Hessian matrices in $6N$-11 spatial points in the vicinity of the PES minimum. The calculated derivatives are then treated as perturbations to the harmonic potential, and this problem is solved by means of second-order

perturbational theory. As a result, the anharmonic matrix χ_{ij} is constructed, which allows calculating the fundamental frequencies, corrected for anharmonicity

$$\nu_i = \omega_i + 2\chi_{ii} + \frac{1}{2} \sum_{j=1, j\neq i}^{N} \chi_{ij} \ .$$

Here, ν_i is the VPT2-corrected fundamental frequency and ω_i is the harmonic frequency. In the same manner the frequencies of overtone and combinational bands can be calculated, together with their anharmonic intensities [18]. The VPT2 approach is part of the quantum-chemistry package Gaussian 16 [30].

References

[1] F. Jensen, *Introduction to Computational Chemistry*, John Wiley & Sons Ltd, England, **2007**.

[2] R. Woolley, B. Sutcliffe, "Molecular structure and the Born-Oppenheimer approximation", *Chem. Phys. Lett.* **1977**, *45*, 393 –398.

[3] J. C. Slater, "Atomic Shielding Constants", *Phys. Rev.* **1930**, *36*, 57–64.

[4] "Electronic wave functions - I. A general method of calculation for the stationary states of any molecular system", *Proceedings of the Royal Society of London A: Mathematical Physical and Engineering Sciences* **1950**, *200*, 542–554.

[5] P. Hohenberg, W. Kohn, "Inhomogeneous Electron Gas", *Phys. Rev.* **1964**, *136*, B864–B871.

[6] H. S. Yu, S. L. Li, D. G. Truhlar, "Perspective: Kohn-Sham density functional theory descending a staircase", *The Journal of Chemical Physics* **2016**, *145*, 130901.

[7] W. Kohn, L. J. Sham, "Self-Consistent Equations Including Exchange and Correlation Effects", *Phys. Rev.* **1965**, *140*, A1133–A1138.

[8] G. Rauhut, P. Pulay, "Transferable Scaling Factors for Density Functional Derived Vibrational Force Fields", *J. Phys. Chem.* **1995**, *99*, 3093–3100.

[9] P. Sinha, S. E. Boesch, C. Gu, R. A. Wheeler, A. K. Wilson, "Harmonic Vibrational Frequencies: Scaling Factors for HF, B3LYP, and MP2 Methods in Combination with Correlation Consistent Basis Sets", *J. Phys. Chem. A* **2004**, *108*, 9213–9217.

[10] J. Baker, A. A. Jarzecki, P. Pulay, "Direct Scaling of Primitive Valence Force Constants: An Alternative Approach to Scaled Quantum Mechanical Force Fields", *J. Phys. Chem. A* **1998**, *102*, 1412–1424.

[11] C. Fabri, T. Szidarovszky, G. Magyarfalvi, G. Tarczay, "Gas-Phase and Ar-Matrix SQM Scaling Factors for Various DFT Functionals with Basis Sets Including Polarization and Diffuse Functions", *J. Phys. Chem. A* **2011**, *115*, 4640–4649.

[12] Y. Bouteiller, J.-C. Gillet, G. Gregoire, J. P. Schermann, "Transferable Specific Scaling Factors for Interpretation of Infrared Spectra of Biomolecules from Density Functional Theory", *J. Phys. Chem. A* **2008**, *112*, 11656–11660.

[13] J. VandeVondele, M. Krack, F. Mohamed, M. Parrinello, T. Chassaing, J. Hutter, "Quickstep: Fast and accurate density functional calculations using a mixed Gaussian and plane waves approach", *Comput. Phys. Commun.* **2005**, *167*, 103 –128.

[14] M.-P. Gaigeot, "Theoretical spectroscopy of floppy peptides at room temperature. A DFTMD perspective: gas and aqueous phase", *Phys. Chem. Chem. Phys.* **2010**, *12*, 3336–3359.

[15] M. Thomas, M. Brehm, R. Fligg, P. Vohringer, B. Kirchner, "Computing vibrational spectra from ab initio molecular dynamics", *Phys. Chem. Chem. Phys.* **2013**, *15*, 6608 –6622.

[16] R. D. Amos, N. C. Handy, W. H. Green, D. Jayatilaka, A. Willetts, P. Palmieri, "Anharmonic vibrational properties of CH2F2 : A comparison of theory and experiment", *J. Chem. Phys.* **1991**, *95*, 8323.

[17] V. Barone, "Anharmonic vibrational properties by a fully automated second-order perturbative approach", *J. Chem. Phys.* **2005**, *122*, 014108.

[18] V. Barone, M. Biczysko, J. Bloino, "Fully anharmonic IR and Raman spectra of medium-size molecular systems: accuracy and interpretation", *Phys. Chem. Chem. Phys.* **2014**, *16*, and references therein, 1759–1787.

[19] T. K. Roy, R. B. Gerber, "Vibrational self-consistent field calculations for spectroscopy of biological molecules: new algorithmic developments and applications", *Phys. Chem. Chem. Phys.* **2013**, *15*, 9468–9492.

[20] S. Jaeqx, J. Oomens, A. Cimas, M.-P. Gaigeot, A. M. Rijs, "Gas-Phase Peptide Structures Unraveled by Far-IR Spectroscopy: Combining IR-UV Ion-Dip Experiments with Born-Oppenheimer Molecular Dynamics Simulations", *Angewandte Chemie International Edition*, *53*, 3663–3666.

[21] J. Mahé, D. J. Bakker, S. Jaeqx, A. M. Rijs, M.-P. Gaigeot, "Mapping gas phase dipeptide motions in the far-infrared and terahertz domain", *Phys. Chem. Chem. Phys.* **2017**, *19*, 13778–13787; and personal communication with authors.

[22] J. Mahe, S. Jaeqx, A. M. Rijs, M.-P. Gaigeot, "Can far-IR action spectroscopy combined with BOMD simulations be conformation selective?", *Phys. Chem. Chem. Phys.* **2015**, *17*, 25905–25914; and personal communication with authors.

[23] L. Pele, R. B. Gerber, "On the number of significant mode-mode anharmonic couplings in vibrational calculations: Correlation-corrected vibrational self-consistent field treatment of di-, tri-, and tetrapeptides", *J. Chem. Phys.* **2008**, *128*, 165105.

[24] G. P. Moss, "Basic terminology of stereochemistry (IUPAC Recommendations 1996)", *Pure and Applied Chemistry* **2009**, *68*, 2193–2222.

[25] G. Chang, W. C. Guida, W. C. Still, "An internal-coordinate Monte Carlo method for searching conformational space", *Journal of the American Chemical Society* **1989**, *111*, 4379–4386.

[26] T. Häber, C. Jakobi, Random Structure Generator.

[27] J. J. P. Stewart, MOPAC2009, Stewart Computational Chemistry, Colorado Springs, CO, USA, `http://openmopac.net/`, **2008**.

[28] J. Řezáč, P. Hobza, "Advanced Corrections of Hydrogen Bonding and Dispersion for Semiempirical Quantum Mechanical Methods", *Journal of Chemical Theory and Computation* **2012**, *8*, 141–151.

[29] G. Fogarasi, X. Zhou, P. W. Taylor, P. Pulay, "The calculation of ab initio molecular geometries: efficient optimization by natural internal coordinates and empirical correction by offset forces", *Journal of the American Chemical Society* **1992**, *114*, 8191–8201.

[30] M. J. Frisch et al., Gaussian 16 Revision A.03, Gaussian Inc. Wallingford CT, **2016**.

[31] A. D. Becke, "Density functional thermochemistry. III. The role of exact exchange", *J. Chem. Phys.* **1993**, *98*, 5648–5652.

[32] S. Grimme, "Semiempirical GGA-type density functional constructed with a long-range dispersion correction", *Journal of Computational Chemistry*, *27*, 1787–1799.

[33] S. Grimme, J. Antony, S. Ehrlich, H. Krieg, "A consistent and accurate ab initio parametrization of density functional dispersion correction (DFT-D) for the 94 elements H-Pu", *J. Chem. Phys.* **2010**, *132*, 154104.

[34] S. Grimme, S. Ehrlich, L. Goerigk, "Effect of the damping function in dispersion corrected density functional theory", *Journal of Computational Chemistry*, *32*, 1456–1465.

[35] C. Adamo, V. Barone, "Toward reliable density functional methods without adjustable parameters: The PBE0 model", *The Journal of Chemical Physics* **1999**, *110*, 6158–6170.

[36] F. A. Hamprecht, A. J. Cohen, D. J. Tozer, N. C. Handy, "Development and assessment of new exchange-correlation functionals", *The Journal of Chemical Physics* **1998**, *109*, 6264–6271.

[37] Y. Zhao, D. G. Truhlar, "The M06 suite of density functionals for main group thermochemistry, thermochemical kinetics, noncovalent interactions, excited states, and transition elements: two new functionals and systematic testing of four M06-class functionals and 12 other functionals", *Theoretical Chemistry Accounts* **2008**, *120*, 215–241.

[38] J.-D. Chai, M. Head-Gordon, "Long-range corrected hybrid density functionals with damped atom–atom dispersion corrections", *Phys. Chem. Chem. Phys.* **2008**, *10*, 6615–6620.

[39] J. P. Perdew, W. Yue, "Accurate and simple density functional for the electronic exchange energy: Generalized gradient approximation", *Phys. Rev. B* **1986**, *33*, 8800–8802.

[40] A. D. Becke, "A new mixing of Hartree-Fock and local density-functional theories", *The Journal of Chemical Physics* **1993**, *98*, 1372–1377.

[41] T. Janowski, P. Pulay, "High accuracy benchmark calculations on the benzene dimer potential energy surface", *Chemical Physics Letters* **2007**, *447*, 27 –32.

[42] H. Valdes, K. Pluháčková, M. Pitonák, J. Řezáč, P. Hobza, "Benchmark database on isolated small peptides containing an aromatic side chain: comparison between wave function and density functional theory methods and empirical force field", *Phys. Chem. Chem. Phys.* **2008**, *10*, 2747–2757.

[43] K. E. Riley, M. Pitoňák, P. Jurečka, P. Hobza, "Stabilization and Structure Calculations for Noncovalent Interactions in Extended Molecular Systems Based on Wave Function and Density Functional Theories", *Chemical Reviews* **2010**, *110*, 5023–5063.

[44] J. A. Montgomery, M. J. Frisch, J. W. Ochterski, G. A. Petersson, "A complete basis set model chemistry. VII. Use of the minimum population localization method", *The Journal of Chemical Physics* **2000**, *112*, 6532–6542.

[45] L. A. Curtiss, P. C. Redfern, K. Raghavachari, "Gaussian-4 theory using reduced order perturbation theory", *The Journal of Chemical Physics* **2007**, *127*, 124105.

Chapter 4

Summary of the Results

4.1 Far-infrared studies of aminophenol isomers

This section summarizes the studies of far-IR spectra of the aminophenol molecule, presented in Paper [I]. The main focus of this work was to investigate and assign isomer- and conformer-specific low-frequency vibrational bands associated with the nuclear motion of the phenyl ring and the two important functional groups, the hydroxyl group (OH) and the amino-group (NH_2). The studies were motivated by the sparsity of information about such far-IR vibrations, implying that these vibrations are often excluded from molecular structural analysis based on IR spectroscopy. Strong anharmonicity and a high degree of mode-coupling of low-frequency vibrations is a primary contributor to this problem, since it complicates the theoretical description of far-IR spectra. To address this issue we have used aminophenol far-IR spectra measured under cooled gas-phase conditions as a benchmark to evaluate the efficiency of DFT frequency calculations.

The experimental far-IR spectra (Fig. 3 of Paper [I]), measured in the range of 220-800 cm^{-1} with IR-UV ion-dip spectroscopy and by employing the free electron laser FELIX, showed a wealth of resolved spectral features specific to the different aminophenol isomers (see Fig. 4.1). The most pronounced differences were found in the fundamental transitions corresponding to the phenyl ring out-of plane (o.p.) vibrations, CH o.p. vibrations, and the torsional vibrations of the OH and NH_2 functional groups. These transitions have both different frequencies and intensities for different aminophenol isomers.

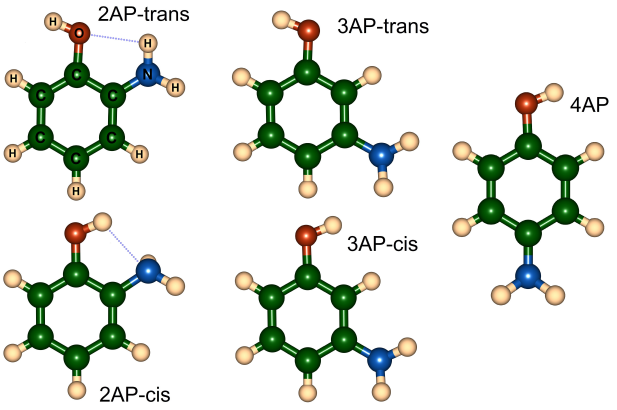

Figure 4.1: Optimized geometries of aminophenol isomers, namely 2-AP (*trans* and *cis* conformers), 3-AP (*trans, cis*), and 4-AP. The hydrogen atoms of the amino-group (NH_2) are positioned out of plane with respect to the aromatic ring. Geometry optimization was performed with the B3LYP/aug-cc-pVTZ method.

As the experimental spectra were obtained in a conformer-selective manner, we were also able to study the differences between the far-IR spectral features of *trans*- and *cis*- 3-aminophenol. Despite the minor differences in the structure (OH group pointing towards or away from the NH_2 moiety), these conformers were distinguished by their far-IR vibrational features (see Fig. 4.2). In this case, most of the spectral variations originate from the OH and NH_2 torsional vibrations and CH o.p. wagging vibrations, whereas less pronounced differences were observed for NH_2 wagging and CO in-plane (i.p.) bending vibrations. In the case of the 2-aminophenol molecule, only one conformer was experimentally observed. The experimental far-IR spectra strongly supported an assignment to the *trans*-conformer, which is in agreement with an IR-UV ion dip spectroscopy study in the mid-IR region [1].

Theoretical predictions of the gas-phase spectra of aminophenol were performed with DFT frequency calculations, both within the double harmonic approximation and within the anharmonic VPT2 approach. Comparison of calculations to the experimental spectra allowed us not only to assign the observed vibrational features, but also to evaluate the accuracy of the most common density functionals and basis sets for vibrational assignments in

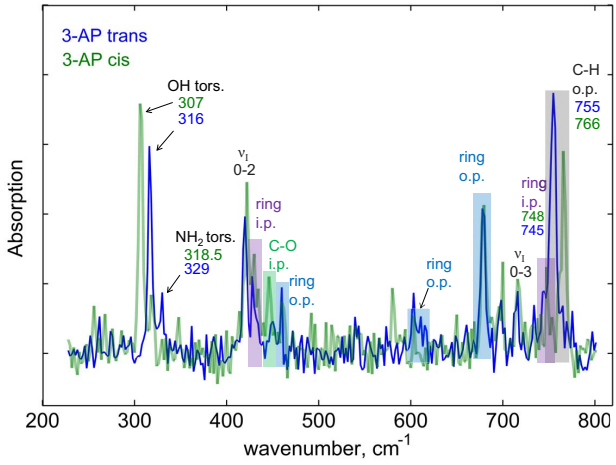

Figure 4.2: Experimental far-IR absorption spectra of *trans* and *cis* 3-aminophenol in the range of 220-800 cm^{-1}, together with assignments of fundamental vibrational transitions. The ring o.p. transitions are marked in blue, ring i.p. - in pink, C-H o.p. wagging - in grey, C-O i.p. - in green. The vibrational transitions of the NH_2 inversion mode are denoted as ν_I (0-2 and 0-3). This figure is reproduced with permission from [Phys. Chem. Chem. Phys., 2016, 18, 6275-6283].

the far-IR region. Such an evaluation was needed in order to establish if conventional DFT frequency calculations can overcome the problem of anharmonicity and mode-coupling in far-IR spectroscopy. Our study showed that the anharmonic VPT2 approach works reasonably well for the vibrational modes with low anharmonicity and improves the accuracy significantly with respect to the conventional harmonic approximation. In contrast, when the anharmonicity or the degree of mode-coupling is very high, such as in the case of the NH_2 wagging vibration, the VPT2 approach does not lead to a satisfactory prediction transition frequencies and intensities. Table 4.1 gives an overview of the performance of the VPT2 approach and presents assignments for the most important vibrational transitions observed in our experiments. The phenyl ring vibrations and CO, CN in-plane bending vibrations, having weak anharmonicity, are described very well by the anharmonic VPT2 approach. The torsional vibrations of the OH and

Table 4.1: Experimentally observed vibrations of 4-aminophenol (4-AP), 3-aminophenol (3-AP), and 2-aminophenol (2-AP), including their assignment. The right-most column outlines the degree of anharmonicity, and the efficiency of the anharmonic VPT2 approach for a particular vibrational motion.

Vibration character	Experimental frequencies				Comment about anharmonicity and VPT2 performance
	4-AP	trans 3-AP	cis 3-AP	trans 2-AP	
ring breathing	-	745	748	767	weak anharmonicity, VPT2 describes well
CH o.p. wagging	792	755	766	735.5	weak anharmonicity, VPT2 describes well
CCC i.p. bending	759.5	432	434	542	strong anharmonicity except for 4-AP, due to NH_2 wag. contribution
	645.5	427	430	486	
	472	-	-	-	
ring puckering	676.5	678	679.5	748.5	high anharmonicity, satisfactory description with VPT2
NH_2 wagging overtone 0-2	467	419	422	437	strong anharmonicity, VPT2 not applicable
CCC o.p. bending	422	612	604	501	weak anharmonicity, VPT2 describes well
	502	459	446	445.5	
CO, CN i.p. bending	326.5	325	312	303	weak anharmonicity, VPT2 describes well
NH_2 torsion	237	329	318.5	323	high anharmonicity, satisfactory description with VPT2
OH torsion	254.5	316	307	286.5	high anharmonicity, satisfactory description with VPT2

NH_2 groups, and the ring puckering vibration have a high degree of anharmonicity, but nevertheless were satisfactory described by the VPT2 approach. We also found that different combinations of density functionals and basis sets produced different anharmonic corrections, with the best accuracy achieved with the functionals B3LYP, B3PW91, B3LYP-D3 and double-zeta basis sets of moderate size.

The strongly anharmonic NH_2 wagging (inversion) vibration

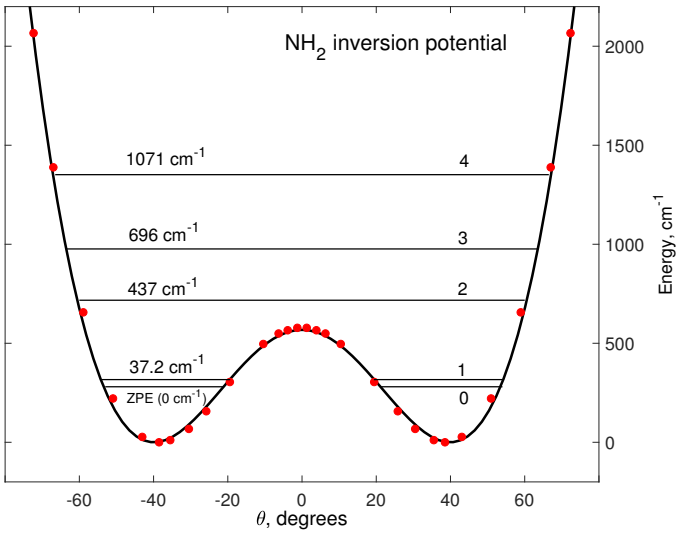

Figure 4.3: NH_2 inversion potential of *trans* 2-aminophenol, obtained from a DFT relaxed PES scan (red dots), and by least squares fitting of the DFT and experimental data to the double-minimum potential model with a gaussian barrier (black line).

required some separate treatment, as the potential energy surface describing this motion has two minima separated by a relatively low barrier [2, 3]. This leads to large tunneling (inversion) splittings of the vibrational energy levels. As a result, several transitions between the tunneling doublet states of the ground state (denoted as 0 and 1) and tunneling doublet states of the first excited state (denoted as 2 and 3) are observed in the frequency range below 800 cm^{-1}. In order to describe the experimental transitions of the NH_2 wagging in aminophenol we have applied the model of a double-minimum harmonic well with a gaussian barrier [4] and a variational treatment. In this approach the energy levels are found variationally using the basis set of the harmonic oscillator wavefunctions, for the potential energy function of the form

$$V(Q) = \frac{1}{2}\lambda Q^2 + A\exp(-a^2Q^2), \tag{4.1}$$

where Q is a mass adjusted coordinate defined by $2T = \dot{Q}^2$ (T is the kinetic energy of the vibrational motion). By using the experimental frequencies of the NH_2 inversion observed for *trans*

and *cis* 3-aminophenol, we obtained the parameters of the potential energy function, and the barriers to inversion. In the case of 4-aminophenol and 2-aminophenol, for which less experimental transitions were observed, we applied a different approach. First, we calculated the potential energy profile governing the NH_2 inversion motion by means of a relaxed potential energy scan using DFT. Then, a trial potential function (eqn. 4.1) was optimized with the least squares method to best describe the DFT potential energy profile, as well as the frequencies of the 0–2 and 0–3 transitions observed experimentally. The result obtained for *trans* 2-aminophenol is presented in Fig. 4.3, demonstrating the mutual agreement between the calculated DFT and the experimental data. It was also found that the vibrational energy levels obtained only from the DFT potential energy profile were in satisfactory agreement with the experimental NH_2 inversion transitions.

In summary, gas-phase far-IR spectroscopy allowed us to study the low-frequency vibrations of aminophenol, which were found to be isomer- and conformer-specific. Comparison of experimental and theoretical spectra has shown that the far-IR vibrations with moderate anharmonicity and mode-coupling are satisfactorily explained by means of an anharmonic VPT2 treatment. For the strongly anharmonic NH_2 inversion vibration, the model of double-minimum potential with a gaussian barrier resulted in satisfactory description of the experimental spectra.

4.2 Far-infrared amide IV-VI spectroscopy: the case of methylacetanilides

In this section, the results of Paper [II] are summarized. Our investigation was devoted to the fundamental far-IR vibrations of a peptide link, the -CO-NH- moiety, in the model peptide molecule Methylacetanilide (MA). So far, little is known about far-IR vibrations of biomolecules due to their lower absorption cross-sections and more challenging theoretical treatment in comparison with conventional mid-IR studies. However, the delocalized and anharmonic nature of far-IR vibrations carries a wealth of information about the molecular structure. Thus, the extension of well-established mid-IR spectroscopy into the far-IR and THz ranges will cover all types of molecular vibrations, hence revealing precise structural information. Moreover, for large molecules, the mid-IR range can suffer from spectral congestion, leading only

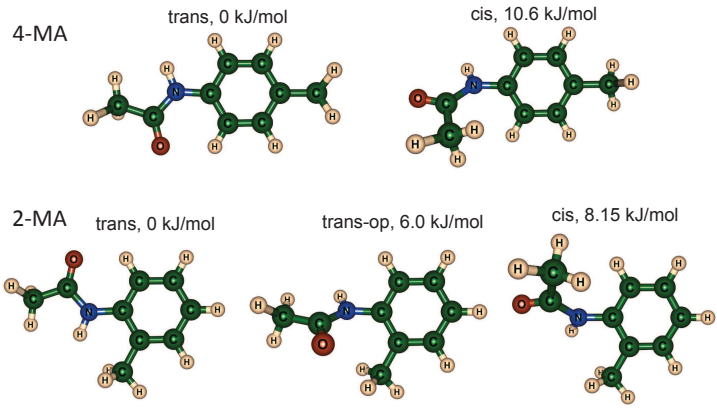

Figure 4.4: Optimized geometries and corresponding energies of the conformers of 4-methylAcetanilide (4-MA) and 2-methylAcetanilide (2-MA), calculated with the B3LYP density functional and the N07D basis set. The conformer energies are given in respect to the *trans* conformers.

to families of structures that can be assigned in the experimental spectra. In this case, the information acquired from the far-IR spectra can be indispensable.

The MA molecule (Fig. 4.4) can be considered as a simple peptide model containing a single peptide link, the -CO-NH- moiety. The peptide link in MA connects a methyl group with a substituted aromatic ring (methylphenyl group). The aromatic ring acts as a UV absorption chromophore in the IR-UV ion-dip technique, enabling measurement of conformer-specific IR spectra. Two different isomeric configurations of MA were studied, 2-MA and 4-MA (see Fig. 4.4). The -CO-NH- moiety can exist in two distinct, nearly planar configurations, either *trans* or *cis*. In the case of 4-MA, this results in two geometries (see Fig. 4.4), which have a significant difference in energy. In the case of 2-MA, where the substituent methyl group is adjacent to the acetamide group, steric interactions lead to the existence of the third conformer, with the -CO-NH- moiety of *trans* character, but oriented out of plane with respect to the aromatic ring. This conformer has a non-zero dihedral angle ($\approx 60°$) between the -CO-NH- moiety and the ring planes, and we call it *trans-op* 2-MA. Moreover, for this conformer, the -CO-NH- moiety deviates from planarity by $\approx 10°$ (B3LYP/N07D geometry). The influence of this structural feature on the far-IR spectra is particularly interesting, as deviation from

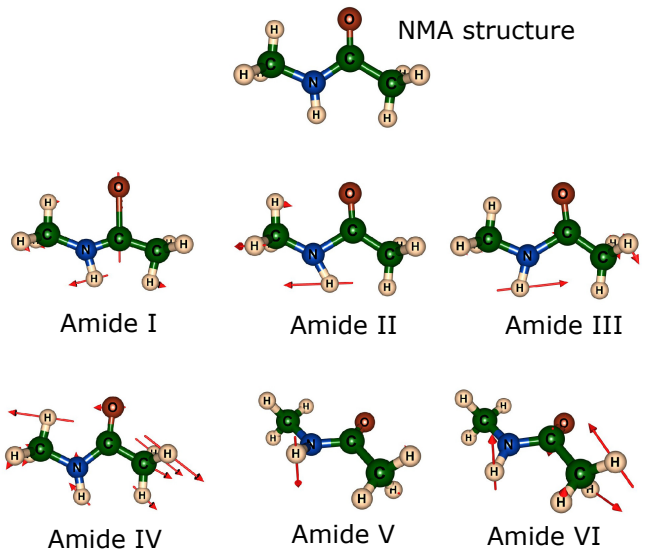

Figure 4.5: Graphical representation of the Amide normal modes of N-Methylacetamide (NMA), shown with scaled vectors of the vibrational displacement.

planarity is quite common in proteins [5, 6].

The fundamental vibrations of a peptide link, the so called Amide band vibrations, are illustrated in Fig. 4.5 for the simplest peptide model, N-methylacetamide (NMA). In this work we focus on the Amide IV-VI vibrations, which have frequencies in the far-IR range. The Amide IV vibration involves CO in-plane (i.p.) bending, as well as the CC stretching and the CNC deformation motions. Amide V is mostly characterized by the NH out-of-plane (o.p.) bending vibration, presumably governed by a flat anharmonic potential, and hence expected to be very sensitive to hydrogen bonding. Amide VI is referred to CO o.p. bending with some o.p. displacement of the NH group. In the case of the MA molecule, the Amide IV-VI vibrations can also have contributions from the phenyl ring.

Using the IR-UV ion-dip technique, we have studied the mid-IR and far-IR spectra of two isomers of the MA molecule, 2-MA and 4-MA. Each isomer showed predominant existence of a single conformer with *trans* arrangement of the peptide link. The comparison between the measured far-IR spectra of *trans* 2-MA and

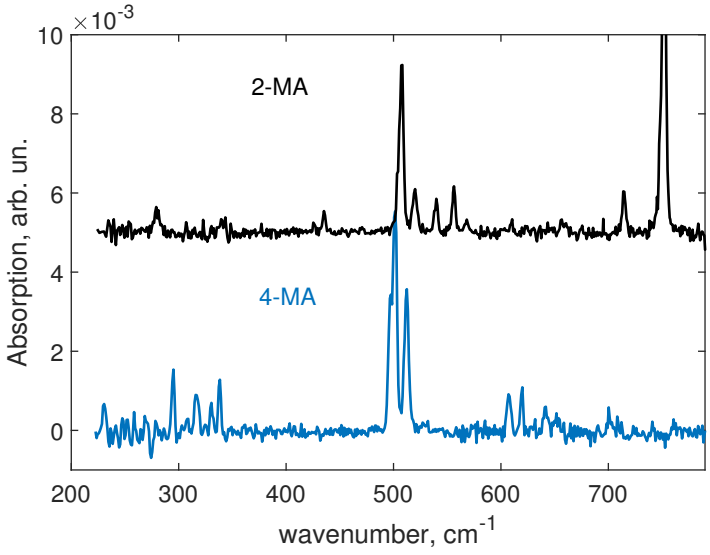

Figure 4.6: Experimental far-IR absorption spectra of *trans* 2-MA and 4-MA.

4-MA are shown in Fig. 4.6. It can be seen that the two isomers have distinct far-IR spectra, which confirms the previous conclusion about isomer-specificity of the low-frequency vibrations in the far-IR region drawn for aminophenol (section 4.1, Paper [I]).

It should be noted that the non-observation of the *trans-op* conformer of 2-MA can be related not only to its low population in the molecular beam, but also to its low energy barrier to interconversion. Indeed, the transition state that connects the *trans-op* and *trans* structures, found with the QST3 algorithm [7], is just 403 cm^{-1} above the energy of the *trans-op* structure ($\Delta G_{\mathrm{G4MP2}}$(15 K)). Such a barrier height is lower than the critical value of 700-800 cm^{-1} [8, 9], which indicates that efficient relaxation of the *trans-op* conformer to the *trans* one can occur in our seeded argon supersonic-jet.

Fig. 4.7 shows the comparison between the experimental far-IR spectrum of the main conformer of 2-MA and the theoretical spectra of all possible conformers that this molecule can assume. This comparison revealed several important aspects. First, the calculated spectra are in a very good agreement with the experimental data of the observed conformer, allowing us to assign it to the *trans* geometry, as well as to make a direct vibrational

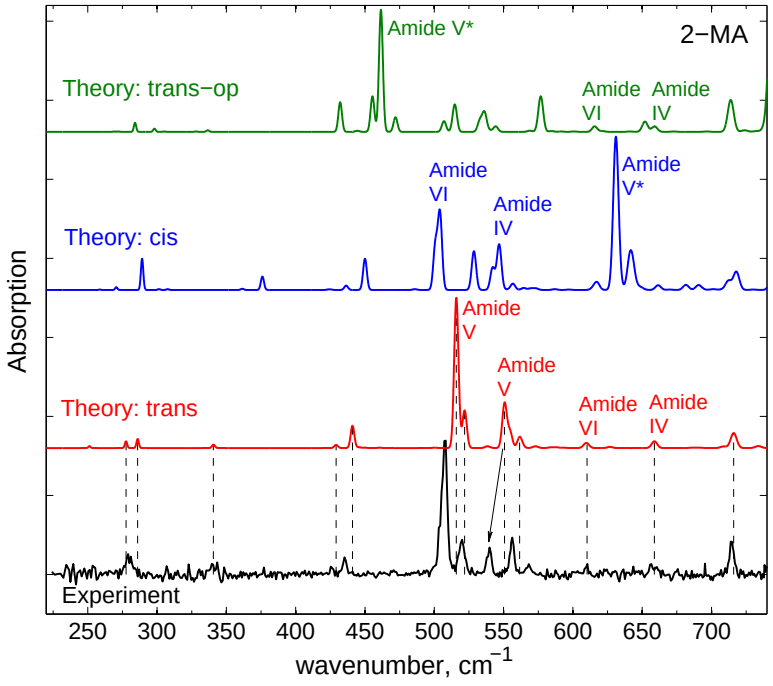

Figure 4.7: Experimental far-IR absorption spectra (in black) of the observed conformer of 2-MA, assigned to the planar *trans* structure. The spectra of all possible conformers, calculated with the VPT2 anharmonic treatment at the B3LYP/N07D level of theory, are shown for comparison. The vertical dashed lines denote the position of the fundamental theoretical bands for the *trans* geometry. The marked theoretical NH o.p. bands (Amide V*) were reduced in intensity by a factor of 2. Figure is reproduced with permission from [J. Chem. Phys. 145, 104309 (2016)].

assignment of the observed far-IR bands. Second, as can be seen from Fig. 4.7, the Amide IV-VI bands are conformer-specific, showing strong differences between the spectra of the possible conformers of 2-MA (see Fig. 4.4). The Amide V, the strongest band, shows the highest sensitivity to the structure of the peptide link. It is predicted to be red-shifted for the *trans-op* conformer, and strongly blue-shifted for the *cis* conformer with respect to the observed *trans* feature. The Amide IV and VI bands show the highest sensitivity to the *trans* or *cis* configuration of the peptide link, whereas their predicted positions and intensities in the case

of the *trans-op* and *trans* structures are very similar. Third, several other vibrations involving the peptide link were identified, such as CCO i.p. bending, CCN deformation, and CNC deformation vibrations. We found that their calculated frequencies do not show large variations between the conformers of 2-MA and 4-MA, with exception of some CCN deformation vibrations (see Table I of Paper [II]).

In summary, our study of the far-IR specta of methylacetanilide revealed that the Amide IV-VI vibrations are very sensitive to the structure of the peptide link and the molecular backbone. Therefore, far-IR spectroscopy can be an efficient extension to the well-established mid-IR spectroscopy for structural analysis of biomolecules.

4.3 IRMPD-VUV action spectroscopy: the case of N-methylacetamide

This section is devoted to a novel alternative of IR action spectroscopy of neutral molecules, presented in Paper [III]. This study was motivated by the limited number of IR spectroscopy methods suitable for structure elucidation of neutral (bio)molecules without an aromatic UV chromophore. The aim of the work was to propose and demonstrate a general approach for vibrational spectroscopy of neutral molecules of arbitrary structure. As a probe of molecular vibrations, the IRMPD method was selected due to its applicability to a broad range of molecules. IRMPD spectroscopy was combined with VUV laser photoionization and time-of-flight mass spectrometry, enabling the analysis of IRMPD dissociation products at each IR wavelength. The N-methylacetamide (NMA) molecule was selected as the simplest peptide analog without an aromatic moiety.

The experiment was performed at the FELIX laboratory, using the experimental setup described in section 2.7. The NMA sample was evaporated using thermal heating at 90°C. The evaporated molecules were cooled by seeding them into a supersonic jet expansion of argon. A skimmer formed a collimated molecular beam, which was crossed with the IR laser beam of the FELIX free electron laser and the VUV laser beam. The estimated interaction time between the FELIX IR light and the molecules was 3 μs. The VUV laser pulse arrived just at the end of the FELIX pulse and ionized the neutral species of the molecular beam: both precursor NMA molecules and their IRMPD fragments (if any) produced

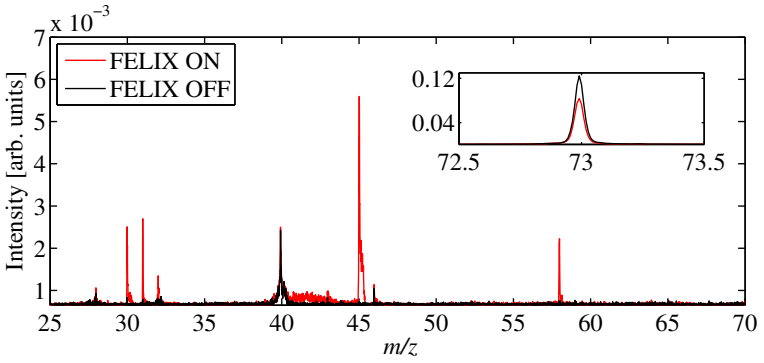

Figure 4.8: Mass spectra of NMA molecules ionized with VUV laser pulses (10.5 eV). The red curve shows the spectrum achieved by first irradiating the molecular beam with the IR laser FELIX tuned to the vibrational transition of NMA at 1708 cm^{-1}. The parent molecular ion peak is shown in the inset. The peak at $m/z \approx 40$ is Ar^+ produced by two-photon VUV ionization. This figure is reproduced with permission from [Phys. Rev. Lett. 117, 118101 (2016)].

by FELIX. The spacial overlap between the two laser beams was optimized to achieve the highest efficiency of the IRMPD process. The IR light frequency was scanned in the range of 1000-1800 cm^{-1}, which covers several fundamental vibrational transitions of NMA. The repetition rate of the FELIX IR laser was half that of the VUV laser, which allowed us to record reference mass spectra of the species present in the molecular beam in absence of the IR light.

The reference VUV mass spectrum (black curve in Fig. 4.8) shows that VUV photoionization predominantly produced parent ions of NMA at mass-to-charge ratio of $m/z = 73$ (the peak at $m/z \approx 40$ is Ar^+). In contrast, when the IR laser light is present and its frequency is resonant with the vibrational transition of NMA (red curve in Fig. 4.8), new peaks at m/z values lower than 73 appear. They can be assigned to neutral dissociation products of NMA. These fragments are produced by the IRMPD process, and are subsequently ionized by the VUV laser. By scanning the IR laser frequency and plotting the summed yield of individual IRMPD fragments ($\sum I_{\text{fragm}}$) normalized to the total ion yield ($\sum I_{\text{fragm}} + I_{\text{parent}}$), the vibrational spectrum of NMA was obtained, and is shown in Fig. 4.9. The experimental spectrum clearly shows

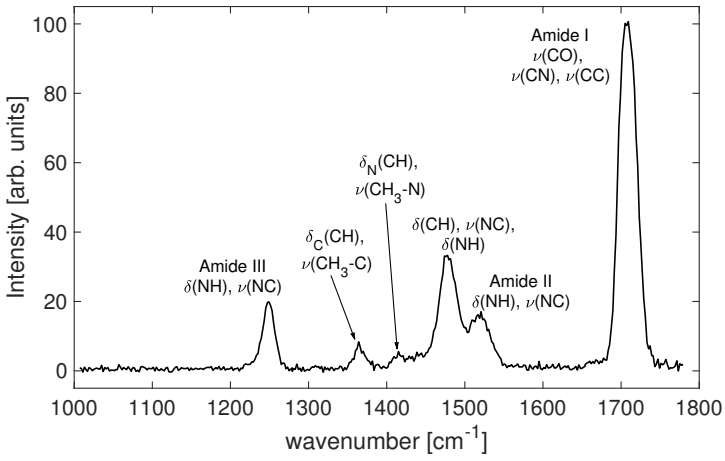

Figure 4.9: IRMPD spectrum of jet-cooled NMA, obtained by plotting the summed yield of individual MPD fragments ($\sum I_{\text{fragm}}$) normalized to the total ion yield ($\sum I_{\text{fragm}} + I_{\text{parent}}$) and to the IR laser power at the corresponding wavelengths. Vibrational mode assignments are taken from [11].

several strong peaks associated with the fundamental vibrations of the NMA molecule in the *trans* configuration, while the *cis* form is presumably too weak to be seen in the experiment. The most prominent vibrational bands can be readily assigned by comparing the spectrum with the available theoretical calculations for *trans* NMA [10, 11].

The experimental IRMPD-VUV spectrum of NMA not only captures the frequencies and intensities of the vibrational transitions, but also the effects of anharmonicity (see section 2.6.2) involved in the multiple photon IRMPD process. It can be seen from the spectrum (Fig. 4.9) that the IRMPD process results in broadening of the vibrational bands of NMA, up to 1.5% (FWHM) of the peak center frequency versus 1% IR laser bandwidth. It was found that the broadening can be somewhat reduced by recoding the spectra at low IR laser power, especially for the strong IR molecular transitions. Some anharmonic red-shifts of the recorded vibrational bands were also observed with respect to the NMA data obtained with one-photon IR spectroscopy [11–13], on average by 0.7% of the band center frequency. Nevertheless, slight red-shifting of all experimental bands generally does not hinder a comparison

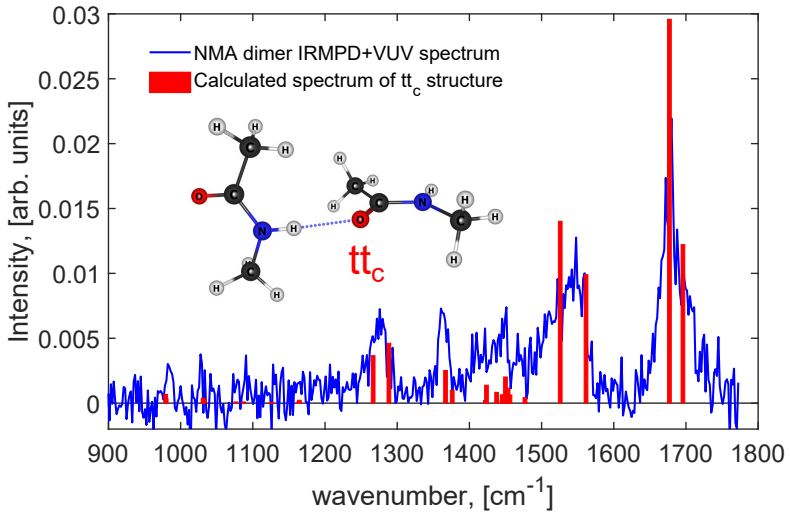

Figure 4.10: IRMPD-VUV depletion spectrum of the jet-cooled NMA dimer, compared with scaled harmonic frequency spectra (B3LYP-D3BJ/6-31++G(d,p), scaling factor 0.975), calculated for one of the lowest energy structures found in Ref. [13].

between the experimental and calculated spectra.

It should be noted that the VUV laser alone does not lead to dissociation of NMA (see Fig. 4.8). This implies that an IRMPD spectrum can be recorded in a background-free manner, using exclusively the mass spectra recorded when the IR laser was on. This aspect eliminates ion signal fluctuations due to variations of the molecular source output and the VUV laser power, which reduces the data acquisition time required to record spectra with sufficient signal-to-noise ratio.

The supersonic-jet cooling of NMA also leads to the formation of clusters, such as dimers and trimers of NMA. By monitoring the depletion of the cluster population in the molecular beam when the IR laser is scanned, their IRMPD-VUV depletion spectra can be obtained. An exemplary spectrum obtained by monitoring the ion signal in the mass channel of NMA dimers is shown in Fig. 4.10. The experimental spectrum agrees well with the scaled harmonic spectrum of the lowest-energy dimer structure (tt_c) published in ref. [13].

In summary, this work has demonstrated that IRMPD-VUV

action spectroscopy is an efficient alternative method for recording IR spectra of gas-phase molecules for which conventional methods are not well-suited. The advantages of the IRMPD-VUV spectroscopy approach, as illustrated in our NMA study, are the following: (1) it allows recording IR spectra of gas-phase molecules of arbitrary structure, in particular lacking an aromatic UV chromophore, (2) background-free IR spectra can be measured owing to negligible fragmentation induced by single-photon VUV ionization, (3) the molecules are cooled in the supersonic-jet expansion, (4) molecular clusters/oligomers can be studied together with the monomers. In comparison with the conventional IR-UV double-resonance method, IRMPD-VUV spectroscopy does not allow recording IR spectra of individual molecular conformers, because the VUV ionization step is not conformer-selective. Hence, IRMPD-VUV spectra represent a combination of vibrational spectra of the conformers populated in the molecular beam. Moreover, due to the multiple photon nature of the IRMPD process, the measured spectra have lower resolution compared to the IR-UV ion-dip method. Nevertheless, as will be shown in the next section, in the cases where conventional methods cannot be applied, the IRMPD-VUV approach can yield valuable spectroscopic signatures of the molecular structures populated in the gas-phase.

4.4 IRMPD-VUV spectroscopy of Gly-Gly and Ala-Ala: folded versus extended conformers

Following the successful demonstration of the IRMPD-VUV approach, the next step was to apply it to spectroscopy of comparatively simple biomolecules without an aromatic UV chromophore. For these studies, presented in Papers [IV,V], the dipeptides glycilglycine (Gly-Gly) and alanylalanine (Ala-Ala) were selected. Glycine and alanine are the simplest proteinogenic amino acids having just a hydrogen (glycine) and a methyl group (alanine) as a side chain (R group). Gas-phase spectroscopy of neutral peptides containing Ala and Gly residues has mainly been limited to those that have an aromatic UV chromophore attached [14, 15], or those that have aromatic amino-acids in their structure [16, 17]. Therefore, spectroscopy of Gly-Gly and Ala-Ala is not only important for getting information on their intrinsic structural preferences, but also because the effect of the aromatic moiety can be studied.

The experimental setup used for IRMPD-VUV spectroscopy of Gly-Gly and Ala-Ala was similar to that applied for NMA (section 4.3), with the difference that the laser-induced thermal desorption method (see section 2.7.1) was applied to transfer the molecules into the gas-phase. Subsequent to laser desorption, the molecules presumably had internal energies corresponding to a temperature range of 300-500 K [18, 19]. Thus, they were seeded into a pulsed supersonic-jet expansion of argon which enabled efficient collisional cooling of their rotational and vibrational degrees of freedom. This cooling process could also modify the initial conformer abundances assumed by the ensemble of laser desorbed molecules, an aspect that will be discussed later together with the results. The skimmer, positioned approximately 30 mm from the jet nozzle, selected the coldest, central part of the expansion region. Another purpose of the skimmer was to form a collimated beam of cold dipeptide molecules, which was intersected by the FELIX IR laser beam and the VUV laser beam, between the repeller and extractor plates of the TOF mass spectrometer. The FELIX laser was scanned in the IR wavelength range of 700-1850 cm^{-1}, producing IRMPD fragments when the IR frequency was resonant with molecular vibrational transitions. Both parent molecules and IRMPD fragments were ionized with the VUV laser pulses arriving just as the FELIX IR pulse ended. The repetition rate of FELIX was half that of the VUV laser, which allowed recording of reference mass spectra without IR pulses at each wavelength step of FELIX. It was found that the VUV photon energy, 10.5 eV, was sufficient to introduce fragmentation in the photoionized state of the parent molecules. These unwanted fragments interfered with the IRMPD products. Nevertheless, the measurement of reference mass spectra without IR light at each IR wavelength step showed that the VUV fragment yield was nearly constant within a FELIX wavelength scan. This allowed us to obtain an IRMPD spectrum as the gain in fragmentation yield just using the "IR on" data (see Methods section of Paper [IV]), which provided a high signal-to-noise ratio similar to the NMA spectroscopy study. The obtained IRMPD spectra were finally IR wavelength calibrated and corrected for the FELIX IR pulse energy dependance versus IR wavelength.

The conformational search and geometry optimization for Gly-Gly and Ala-Ala resulted in many low energy conformers that can potentially be populated in molecular beam experiments. The structural variety for Ala-Ala conformers is presented in Fig. 4.11,

which shows its stable conformers with relative Gibbs free energies below 1500 cm^{-1} for T < 500 K (G4MP2 data). The stable structures of Gly-Gly are similar to those presented for Ala-Ala, with the difference that the methyl R groups are replaced by hydrogen atoms. Moreover, in the case of Gly-Gly the C5-trans± and g-trans-trans± structures have identical energies being enantiomers of each other, and the C5-trans(a)± structures are not stable. Note that the structure notations use a labeling of the hydrogen bonding interactions according to the number of atoms in the ring that is formed by the hydrogen bond, in agreement with the strategy adopted in the literature [20]. For instance, C5 and C7 denote the bonds that form five- and seven-atoms rings, respectively. Such a labeling is useful because the steric repulsion effects associated with the hydrogen bonding generally reduce for larger rings.

As can be seen from Fig. 4.11, many conformers can interconvert between each other just by changing one dihedral angle. It is known from the literature that if the barrier to such interconversion is sufficiently low, efficient conformer relaxation takes place in an argon supersonic jet [8, 9, 21]. Moreover, relaxation from higher to lower energy structure is favored [22–24]. The critical barrier height below which relaxation occurs efficiently depends on many factors, and is assumed to be approximately 700-800 cm^{-1} under experimental conditions similar to ours [8, 9, 24].

In order to evaluate possible relaxation pathways of Gly-Gly and Ala-Ala conformers in our experiment, transition states which connect different conformers were identified. For this purpose, QST2 and QST3 methods [7] were used. Accurate relaxation barrier heights were then calculated based on G4MP2 single point electronic energy calculations for the ωB97X-D/6-311++G(d,p) geometries and harmonic frequencies. The relaxation barriers obtained for Gly-Gly and Ala-Ala conformers are presented in Table 2 and Table 1 of Papers [IV] and [V], respectively. Most of the presented relaxation pathways involve changing only one dihedral angle through a relatively low barrier (<600 cm^{-1}). This implies that these relaxation pathways are efficient in an argon jet. In contrast, the pathways that involve changing several dihedral angles, such as C5C7- $\rightarrow$ C5-trans, exhibit sufficiently large barriers that hinder relaxation. Moreover, it was found that these pathways for Gly-Gly and Ala-Ala can only proceed through a stable intermediate state that lies higher in energy than the relaxing conformer, which also significantly reduces the probability

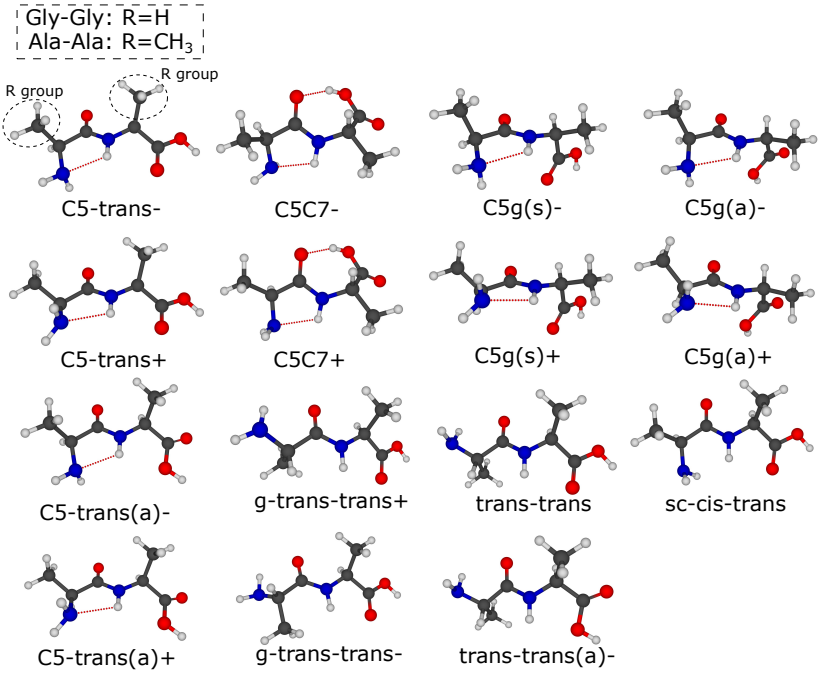

Figure 4.11: The lowest energy conformers of Ala-Ala (R=CH_3) optimized using the ωB97X-D/6-311++G(d,p) method. The conformers of Gly-Gly (R=H) have dihedral angles similar to those shown for Ala-Ala, with the difference that C5-trans$\pm$ and g-trans-trans$\pm$ structures of Gly-Gly are enantiomers of each other and have identical energies. Moreover, in the case of Gly-Gly the C5-trans(a)$\pm$ structures are not stable conformers.

of relaxation. In summary, quantum-chemical calculations predict that among many possible conformers only three have sufficiently high energy barriers that hinder their relaxation in the jet. These conformers include the folded C5C7- structure, stabilized by two relatively strong hydrogen bonds (see Fig. 4.11), and two extended (β-strand like) structures: C5-trans and trans-trans. Both extended structures are more flexible than the C5C7- structure, as they exhibit a notably weak hydrogen bonding interaction at the C-terminus.

The presence and strength of hydrogen bonding interactions can be generally probed by IR spectroscopy. Therefore, the measured IRMPD-VUV spectra of Gly-Gly and Ala-Ala are expected to

provide important structural information about the most abundant species populated in the molecular beam.

We start our discussion of the experimental results by first referring to the IRMPD-VUV spectrum of Gly-Gly, shown in Fig. 4 of paper [IV]. Even shallow comparison of the measured spectrum and the calculated spectra of various lowest-energy conformers indicates that the folded C5C7- structure is clearly not the most abundant species. This conclusion is based on the absence of the red-shifted Amide I band associated with the strong C7 hydrogen bond of this conformer. In contrast, the calculated spectrum of the extended nearly-planar C5-trans structure fits the experiment remarkably well. Non-planar conformers such as C5g-(a) show some agreement with several experimental peaks but do not match the peaks associated with COH bending and CN&CO stretching vibrations that are sensitive to the planarity of the molecular backbone. Moreover, the calculated spectrum of the extended trans-trans structure disagrees in the position of the peaks associated with the NH_2 group, and therefore it is not a good candidate for the most abundant species. Taken together, the analysis indicates that the C5-trans conformer is the most abundant species, providing the best fit with the experimental spectrum. It is also one of the conformers that could not undergo relaxation in the argon jet according to our theoretical analysis presented above. Furthermore, C5-trans has the lowest Gibbs free energy among all the conformers of Gly-Gly in a broad range of temperatures (see Fig. 6(a) of Paper [IV]) relevant for laser desorption.

Despite being the lowest in energy, the C5-trans structure is calculated to constitute less than 40% of the total Boltzmann population for Gly-Gly if relaxation is not taken into account (Fig. 6a of Paper [IV]). This means that if there was no relaxation in the jet, the measured spectrum would be significantly different due to substantial contributions from other conformers. Therefore, the most likely explanation to the observed predominance of the C5-trans structure is the presence of efficient relaxation processes in the supersonic jet that can effectively channel the other conformers into C5-trans. By assuming a complete relaxation of conformers with sufficiently low barriers to interconversion ($<$600 cm^{-1}), a Boltzmann population of 78% is obtained for the C5-trans conformer (Fig. 6b of Paper [IV]), which is now in line with the experimental results of IRMPD-VUV spectroscopy.

In harmony with the results of Gly-Gly spectroscopy, the measured IRMPD-VUV spectrum of Ala-Ala (Fig. 2 of Paper [V]) also showed the most favorable agreement with the calculated spectrum of the extended C5-trans- structure. Similarly, there is no indication of high abundance of the folded C5C7- structure, because the strong Amide I and COH bending bands, expected to shift in frequency upon creation of the C7 hydrogen bond, were not observed in the experimental spectrum. In general, the appearance and the position of the main absorption features in the Ala-Ala spectrum are similar to those of Gly-Gly, except for the bands associated with movement and deformations of the CH_3 groups, which are only present in Ala-Ala.

The calculations for Ala-Ala show that the folded C5C7- conformer is the lowest energy structure, whereas the extended C5-trans- is higher in energy by 195 cm^{-1}, based on zero-point energy corrected electronic energy data from the G4MP2 method. This is in contrast to Gly-Gly, for which these two conformers are almost equal in energy (energy deference of $\approx$20 cm^{-1}). Taking into account Gibbs free energy correction at elevated temperatures (e.g., 300 K) makes the extended C5-trans- structure lower in energy than the folded C5C7- by 100 cm^{-1}, which indicates that the entropy contribution to the stability of C5-trans- is higher than in C5C7-. Nevertheless, the C5-trans- and C5C7- conformers remain comparable in energy, which implies that entropy effect alone cannot explain the prevalence of C5-trans- in the experimental spectrum. Most likely, efficient conformer relaxation processes in the argon jet are responsible for this observation. The extremely low energy barriers, obtained with accurate theoretical treatment (Table 1 of Paper [V]), support this hypothesis. By assuming the complete relaxation of conformers with low barriers to relaxation ($<$600 cm^{-1}), a Boltzmann population of $\approx$75% is obtained for the C5-trans- conformer of Ala-Ala (Fig. 3 of Paper [V]). This prediction now conforms to the experimental results, which shows that careful consideration of relaxation processes in the jet is crucial for obtaining a complete picture of relative stabilities of neutral dipeptides in molecular beams.

In summary, the studies of Gly-Gly and Ala-Ala demonstrated that valuable structural fingerprints, as well as hydrogen bonding interactions can be probed using IRMPD-VUV spectroscopy. Using extensive quantum-chemical calculations, the predominance of the extended C5-trans structure in the experiment was rationalized in terms of its favorable entropy stabilization, as well as

efficient conformer relaxation processes. The lower significance of the folded C5C7- structure, compared to C5-trans, is suggested to be due to its relative rigidity (lower entropy), as well as absence of conformers that can increase its population due to relaxation in the jet.

References

[1] M. C. Capello, M. Broquier, S.-I. Ishiuchi, W. Y. Sohn, M. Fujii, C. Dedonder-Lardeux, C. Jouvet, G. A. Pino, "Fast Nonradiative Decay in o-Aminophenol", *The Journal of Physical Chemistry A* **2014**, *118*, 2056–2062.

[2] R. A. Kydd, P. J. Krueger, "The far-infrared vapour phase spectra of aniline-ND2 and aniline-NHD", *Chem. Phys. Letters* **1977**, *49(3)*, 539.

[3] R. A. Kydd, P. J. Krueger, "The far-infrared vapor phase spectra of some halosubstituted anilines", *J. Chem. Phys.* **1978**, *69(2)*, 827.

[4] J. Coon, N. Naugle, R. McKenzie, "The investigation of double-minimum potentials in molecules", *Journal of Molecular Spectroscopy* **1966**, *20*, 107 –129.

[5] D. S. Berkholz, C. M. Driggers, M. V. Shapovalov, R. L. Dunbrack, P. A. Karplus, "Nonplanar peptide bonds in proteins are common and conserved but not biased toward active sites", *Proceedings of the National Academy of Science* **2012**, *109*, 449–453.

[6] R. Improta, L. Vitagliano, L. Esposito, "Peptide Bond Distortions from Planarity: New Insights from Quantum Mechanical Calculations and Peptide/Protein Crystal Structures", *PLoS ONE* **2011**, *6*, 1–10.

[7] C. Peng, H. Bernhard Schlegel, "Combining Synchronous Transit and Quasi-Newton Methods to Find Transition States", *Israel Journal of Chemistry* **1993**, *33*, 449–454.

[8] P. D. Godfrey, R. D. Brown, F. M. Rodgers, "The missing conformers of glycine and alanine: relaxation in seeded supersonic jets", *Journal of Molecular Structure* **1996**, *376*, 65 –81.

[9] P. D. Godfrey, R. D. Brown, "Proportions of Species Observed in Jet Spectroscopy-Vibrational Energy Effects: Histamine Tautomers and Conformers", *Journal of the American Chemical Society* **1998**, *120*, 10724–10732.

[10] A. L. Kaledin, J. M. Bowman, "Full Dimensional Quantum Calculations of Vibrational Energies of N-Methyl Acetamide", *The Journal of Physical Chemistry A* **2007**, *111*, 5593–5598.

[11] M. P. Gaigeot, R. Vuilleumier, M. Sprik, D. Borgis, "Infrared Spectroscopy of N-Methylacetamide Revisited by ab Initio Molecular Dynamics Simulations", *Journal of Chemical Theory and Computation* **2005**, *1*, 772–789.

[12] M. Albrecht, C. A. Rice, M. A. Suhm, "Elementary Peptide Motifs in the Gas Phase: FTIR Aggregation Study of Formamide, Acetamide, N-Methylformamide, and N-Methylacetamide", *The Journal of Physical Chemistry A* **2008**, *112*, 7530–7542.

[13] T. Forsting, H. C. Gottschalk, B. Hartwig, M. Mons, M. A. Suhm, "Correcting the record: the dimers and trimers of trans-N-methylacetamide", *Phys. Chem. Chem. Phys.* **2017**, *19*, 10727–10737.

[14] J. C. Dean, E. G. Buchanan, T. S. Zwier, "Mixed 14/16 Helices in the Gas Phase: Conformation-Specific Spectroscopy of Z-(Gly)n, n = 1, 3, 5", *J. Am. Chem. Soc.* **2012**, *134*, 17186–17201.

[15] H. Valdes, D. Reha, P. Hobza, "Structure of Isolated Tryptophyl-Glycine Dipeptide and Tryptophyl-Glycyl-Glycine Tripeptide: Ab Initio SCC-DFTB-D Molecular Dynamics Simulations and High-Level Correlated ab Initio Quantum Chemical Calculations", *The Journal of Physical Chemistry B* **2006**, *110*, 6385–6396.

[16] W. Chin, I. Compagnon, J.-P. Dognon, C. Canuel, F. Piuzzi, I. Dimicoli, G. von Helden, G. Meijer, M. Mons, "Spectroscopic Evidence for Gas-Phase Formation of Successive beta-Turns in a Three-Residue Peptide Chain", *Journal of the American Chemical Society* **2005**, *127*, 1388–1389.

[17] W. Chin, F. Piuzzi, J.-P. Dognon, I. Dimicoli, B. Tardivel, M. Mons, "Gas Phase Formation of a 310-Helix in a Three-Residue Peptide Chain: Role of Side Chain-Backbone Interactions as Evidenced by IR-UV Double Resonance Experiments", *Journal of the American Chemical Society* **2005**, *127*, 11900–11901.

[18] M. Handschuh, S. Nettesheim, R. Zenobi, "Is Infrared Laser-Induced Desorption a Thermal Process? The Case of Aniline", *The Journal of Physical Chemistry B* **1999**, *103*, 1719–1726.

[19] R. J. Plowright, E. Gloaguen, M. Mons, "Compact Folding of Isolated Four-Residue Neutral Peptide Chains: H-Bonding Patterns and Entropy Effects", *ChemPhysChem* **2012**, *12*, 1889–1899.

[20] W. Chin, F. Piuzzi, I. Dimicoli, M. Mons, "Probing the competition between secondary structures and local preferences in gas phase isolated peptide backbones", *Phys. Chem. Chem. Phys.* **2006**, *8*, 1033–1048.

[21] R. S. Ruoff, T. D. Klots, T. Emilsson, H. S. Gutowsky, "Relaxation of conformers and isomers in seeded supersonic jets of inert gases", *The Journal of Chemical Physics* **1990**, *93*, 3142–3150.

[22] U. Erlekam, M. Frankowski, G. von Helden, G. Meijer, "Cold collisions catalyse conformational conversion", *Phys. Chem. Chem. Phys.* **2007**, *9*, 3786–3789.

[23] T. F. Miller III, D. C. Clary, A. J.H. M. Meijer, "Collision-induced conformational changes in glycine", *The Journal of Chemical Physics* **2005**, *122*, 244323.

[24] B. Yang, S. Liu, Z. Lin, "Computational study on single molecular spectroscopy of tyrosin-glycine, tryptophane-glycine and glycine-tryptophane", *Scientific Reports* **2017**, *7*, 15869.

Chapter 5

Conclusions and Outlook

In this chapter I would like to present important conclusions of this work and discuss further developments in the field related to the topic of this thesis.

5.1 Far-infrared spectroscopy of isolated molecules

5.1.1 New insights from experiments and theory

The far-IR spectra of aminophenol isomers, studied in **Paper [I]**, gave us extensive information on the low-frequency vibrations of the phenyl ring, and the hydroxyl- and amino-groups. We have shown that anharmonic VPT2 treatment provides a satisfactory description of the far-IR vibrational modes with moderate anharmonicity and mode-coupling. Moreover, the model of double-minimum potential with a gaussian barrier resulted in a reasonable explanation of the experimental data for the NH_2 inversion transitions of aminophenol. The information obtained for aminophenol can be very useful for studies of similar aromatic systems, in terms of vibrational assignment, and in terms of efficient theoretical approaches suitable for tackling vibrational anharmonicity.

Our study of fundamental far-IR vibrations of the peptide link, presented in **Paper [II]**, has shown that Amide IV-VI spectroscopy is a sensitive tool for structural analysis of peptide-like molecules. The Amide V bands are especially promising, being relatively intense and having frequencies that are very sensitive to the structural arrangement of the peptide link. Moreover, the *trans* and *cis* configurations of the peptide link can be directly characterized by their far-IR spectra in the range of 400-800 cm^{-1} due to the large variations in the corresponding Amide IV-VI bands.

This finding is important for the structural characterization of cyclic peptides, where links of the *cis*-type are common [1–5]. In general, gas-phase far-IR spectroscopy combined with quantum chemical calculations, performed in this thesis for various aromatic molecules, has shown that different molecular isomers and conformers have distinct far-IR features that allow precise structural assignment.

5.1.2 Performance of VPT2 for anharmonic treatment of far-infrared vibrations

In this thesis, the VPT2 method was applied for the anharmonic treatment of far-IR vibrations. As gas-phase far-IR spectroscopy allowed a direct comparison between the measured and calculated spectra, we were able to assess the performance of VPT2. This method was found to be reliable for calculations of frequencies and intensities of vibrations with low and moderate anharmonicity. The predictions of strongly anharmonic modes were found to be less reliable, especially in the case of NH_2-inversion vibration governed by a double-well potential. Nevertheless, for the frequency calculations of moderately anharmonic modes the VPT2 method yielded an almost two-fold increase of accuracy compared with the conventional harmonic approximation. Moreover, VPT2 enabled us to calculate overtone and combinational transitions, thus assisting the assignment of the experimental spectra. Based on these results, the VPT2 approach can be recommended for highly accurate calculations of theoretical far-IR spectra for semi-rigid molecules with a low number of strongly anharmonic vibrations.

5.1.3 Outlook

The study of the far-IR spectra of aminophenol (**Paper I**) indicated the importance of the strongly anharmonic NH_2-inversion (wagging) vibration. Its symmetric double-minimum potential originates from the two energetically identical equilibrium geometries that correspond to the two equivalent non-planar arrangements of the amino-group with respect to the aromatic ring of aminophenol. Various biomolecular building blocks, such as amino-acids, peptides and nucleic acid bases, can also have non-planar amino-groups implying that similar effects may be observed in their far-IR spectra. In this respect, it would be particularly interesting to study the far-IR spectra of nucleic acid bases, which have non-planar amino-groups with low barriers to planarity [6–8]. Far-IR

spectroscopy of several dipeptide systems [9–12] indicated strong anharmonicity of the NH_2 wagging vibration, though it was not related to the symmetric double-well potential. Nonetheless, in the case when the barrier to planarity of the amino-group is low, non-symmetric potentials can also lead to unusual energy level structure of the amino-wagging vibration [13].

Quantum-chemical calculations in the Amide IV-VI region (**Paper II**) indicate that that vibrations with Amide V character can be highly sensitive to hydrogen bonding and other weak interactions. In particular, the calculations performed for hydrogen-bonded dimers of N-Methylacetamide predict that the frequency of the Amide V band can be blue-shifted by more than 50% compared with the bare molecule. Moreover, hydrogen bonding of the NH group of 2-methylacetanilide with a water molecule shifts the calculated frequency of Amide V band by 25%. Hence, future experimental and theoretical studies on the application of the Amide IV-VI spectroscopy to structural analysis of hydrogen bonded structures are strongly encouraged.

5.2 IRMPD-VUV action spectroscopy

IRMPD-VUV spectroscopy offers new possibilities for studies of intrinsic structural preferences of neutral biomolecular building blocks. For instance, IR spectroscopy of neutral peptides lacking an aromatic chromophore is now possible, as was demonstrated in Papers [IV-V]. The same is true for carbohydrates, which are an important class of biomolecules lacking an aromatic chromophore, which are even less studied than proteins or peptides. Currently, the structural preferences of neutral carbohydrates are either studied with IR-UV ion-dip spectroscopy after chemical attachment of an aromatic group [14], or by employing rotational spectroscopy combined with laser-ablation technique [15]. The former approach has already generated a considerable insight into the conformational preferences of smaller carbohydrates, and their interactions with several water molecules [14]. IRMPD-VUV spectroscopy can bring new perspectives to such studies, especially because it can shed some light on the effect of the attached aromatic chromophore.

It would certainly be interesting to extend our IRMPD-VUV measurements to the higher frequency region ($3800-2800\ cm^{-1}$), where localized stretching vibrations of hydrogen-bonded and "free" NH and OH groups can be probed, for example. One of

the possibilities to cover this region is to operate the FELIX laser at the third harmonic. Another possibility is to use tunable IR lasers based on nonlinear optical parametric amplification process (OPA). The low-repetition-rate OPA lasers, traditionally used for gas-phase spectroscopy, produce highly intense IR pulses (up to 10 mJ/pulse). In this case, however, ns-long pulses of an OPA laser will result in a reduced efficiency of the IRMPD process, compared with μs-long macropulses of FELIX. Nonetheless, IRMPD-VUV spectroscopy with an IR OPA laser is principally possible, especially in the case of biomolecules with sufficiently high IVR rates. Another option is to use high-repetition or continuous wave tunable IR lasers aligned collinearly with the cold molecular beam to increase the laser-molecule interaction time. Furthermore, the higher IR photon energy in the NH stretch region can introduce measurable variations in the VUV photofragmentation yield, and this mechanism, although different from IRMPD, was already applied for the IR spectroscopy of small aliphatic amino acids [16] and their clusters [17, 18]. It is worth investigating the applicability of this approach to larger biomolecular building blocks such as peptides. This will help to answer the question whether energy deposited by a single IR photon is enough to lead to sufficient changes in fragmentation yields of larger molecular ions. In this respect, the multiple photon IRMPD-VUV technique offers an advantage, as it can be also used to record IR spectra in a broader frequency region covering the Amide I-III and molecular fingerprint ranges. Measurements all the way down to the far-IR range are also possible, particularly for the case of biomolecules with a large number of low-frequency vibrations and high IVR rates.

As was observed for IRMPD-VUV spectroscopy of Gly-Gly and Ala-Ala, the limited spectroscopic resolution can hinder observation of conformers that have minor abundances in the experiment. Moreover, as IRMPD-VUV method records a composite vibrational spectrum of all the abundant conformers, the precise structural and vibrational assignments can be tedious, especially in the case of biomolecules with high structural heterogeneity. In my opinion, this technique can potentially be improved by using a tunable VUV laser ionization source [19]. Several schemes can be employed using tunable IR and VUV lasers, and some of them were already demonstrated in the studies of small molecular species [20]. Their applications to IR spectroscopy of peptides or other biomolecules remain to be demonstrated. The simplest IR-VUV

scheme that can be probably applied to biomolecules requires tuning the VUV laser energy just below the ionization threshold such that the ion signal appears only if the molecules are vibrationally excited by the IR laser [20]. While this double-resonance scheme is not conformer-selective, it offers the possibility of recording single-photon IR spectra, which are better suitable for comparison with DFT frequency calculations than the multiple photon spectra. Conformer selective ionization of several small, jet-cooled molecular species was demonstrated by probing the molecular Rydberg states using tunable VUV laser excitation and pulsed field ionization [21–24]. If applied to laser-desorbed jet-cooled biomolecules, this method could pave the way to high-resolution conformer-selective vibrational spectroscopy of neutral biomolecules lacking an UV chromophore. I hope that the results presented in this thesis will stimulate further developments in the field of structural analysis of biomolecular building blocks.

References

[1] D. F. Mierke, T. Yamazaki, O. E. Said-Nejad, E. R. Felder, M. Goodman, "Cis/trans isomers in cyclic peptides without N-substituted amides", *Journal of the American Chemical Society* **1989**, *111*, 6847–6849.

[2] M. T. Oakley, R. L. Johnston, "Exploring the Energy Landscapes of Cyclic Tetrapeptides with Discrete Path Sampling", *Journal of Chemical Theory and Computation* **2013**, *9*, 650–657.

[3] S. Wiedemann, A. Metsala, D. Nolting, R. Weinkauf, "The dipeptide cyclic(glycyltryptophanyl) in the gas phase: A concerted action of density functional calculations, S0-S1 two-photon ionization, spectral UV/UV hole burning and laser photoelectron spectroscopy", *Phys. Chem. Chem. Phys.* **2004**, *6*, 2641–2649.

[4] A. P. Wickrama Arachchilage, F. Wang, V. Feyer, O. Plekan, K. C. Prince, "Photoelectron spectra and structures of three cyclic dipeptides: PhePhe, TyrPro, and HisGly", *The Journal of Chemical Physics* **2012**, *136*, 124301, and refs. therein.

[5] A. G. Abo-Riziq, B. Crews, J. E. Bushnell, M. P. Callahan, M. S. D. Vries, "Conformational analysis of cyclo(Phe-Ser) by UV-UV and IR-UV double resonance spectroscopy and ab initio calculations", *Molecular Physics* **2005**, *103*, 1491–1495.

[6] S. Wang, H. F. Schaefer, "The small planarization barriers for the amino group in the nucleic acid bases", *The Journal of Chemical Physics* **2006**, *124*, 044303.

[7] J. Šponer, J. Florián, P. Hobza, J. Leszczynski, "Nonplanar DNA Base Pairs", *Journal of Biomolecular Structure and Dynamics* **1996**, *13*, 827–833.

[8] O. Bludsky, J. Sponer, J. Leszczynski, V. Spirko, P. Hobza, "Amino groups in nucleic acid bases, aniline, aminopyridines, and aminotriazine are nonplanar: Results of correlated abinitio quantum chemical calculations and anharmonic analysis of the aniline inversion motion", *J. Chem. Phys.* **1996**, *105*, 11042–11050.

[9] M.-P. Gaigeot "THz spectroscopic probing of gas phase molecules structures: combined IR-UV ion dip experiments and DFT-MD simulations" in The 10th Isolated Biomolecules and Biomolecular Interactions Conference, 2018, Texel, The Netherlands.

[10] J. Mahé, D. J. Bakker, S. Jaeqx, A. M. Rijs, M.-P. Gaigeot, "Mapping gas phase dipeptide motions in the far-infrared and terahertz domain", *Phys. Chem. Chem. Phys.* **2017**, *19*, 13778–13787; and personal communication with authors.

[11] S. Jaeqx, J. Oomens, A. Cimas, M.-P. Gaigeot, A. M. Rijs, "Gas-Phase Peptide Structures Unraveled by Far-IR Spectroscopy: Combining IR-UV Ion-Dip Experiments with Born-Oppenheimer Molecular Dynamics Simulations", *Angewandte Chemie International Edition*, *53*, 3663–3666.

[12] J. Mahe, S. Jaeqx, A. M. Rijs, M.-P. Gaigeot, "Can far-IR action spectroscopy combined with BOMD simulations be conformation selective?", *Phys. Chem. Chem. Phys.* **2015**, *17*, 25905–25914; and personal communication with authors.

[13] K. H. Hughes, J. N. Macdonald, "Boltzmann wavepacket dynamics of tunnelling of molecules through symmetric and asymmetric energy barriers on non-periodic potential functions", *Phys. Chem. Chem. Phys.* **2000**, *2*, 3539–3547.

[14] E. J. Cocinero, P. Çarçabal in *Gas-Phase IR Spectroscopy and Structure of Biological Molecules*, (Eds.: A. M. Rijs, J. Oomens), Springer International Publishing, Cham, **2015**, pp. 299–333.

[15] E. J. Cocinero, A. Lesarri, P. Écija, F. J. Basterretxea, J.-U. Grabow, J. A. Fernàndez, F. Castaño, "Ribose Found in the Gas Phase", *Angewandte Chemie International Edition* **2012**, *51*, 3119–3124.

[16] Y. Hu, E. R. Bernstein, "Vibrational and photoionization spectroscopy of biomolecules: Aliphatic amino acid structures", *The Journal of Chemical Physics* **2008**, *128*, 164311.

[17] Y. Hu, E. R. Bernstein, "Vibrational and Photoionization Spectroscopy of Neutral Valine Clusters", *The Journal of Physical Chemistry A* **2009**, *113*, PMID: 19585978, 8454–8461.

[18] Y. Hu, J. Guan, E. R. Bernstein, "Mass-selected IR-VUV (118 nm) spectroscopic studies of radicals, aliphatic molecules, and their clusters", *Mass Spectrometry Reviews* **2013**, *32*, 484–501.

[19] S. Hanna, P. Campuzano-Jost, E. Simpson, D. Robb, I. Burak, M. Blades, J. Hepburn, A. Bertram, "A new broadly tunable (7.4-10.2eV) laser based VUV light source and its first application to aerosol mass spectrometry", *International Journal of Mass Spectrometry* **2009**, *279*, 134 –146.

[20] C.-Y. Ng in *Frontiers of Molecular Spectroscopy*, (Ed.: J. Laane), Elsevier, Amsterdam, **2009**, pp. 659 –691.

[21] S. Choi, T. Y. Kang, K.-W. Choi, S. Han, D.-S. Ahn, S. J. Baek, S. K. Kim, "Conformationally Specific Vacuum Ultraviolet Mass-Analyzed Threshold Ionization Spectroscopy of Alkanethiols: Structure and Ionization of Conformational Isomers of Ethanethiol, Isopropanethiol, 1-Propanethiol, tert-Butanethiol, and 1-Butanethiol", *The Journal of Physical Chemistry A* **2008**, *112*, 7191–7199.

[22] S. T. Park, S. K. Kim, M. S. Kim, "Vacuum-ultraviolet mass-analyzed threshold ionization spectra of iodobutane isomers: Conformer-specific ionization and ion-core dissociation followed by ionization", *The Journal of Chemical Physics* **2001**, *115*, 2492–2498.

[23] Y. R. Lee, M. H. Kim, H. L. Kim, C. H. Kwon, "Conformer-specific photoionization and conformational stabilities of isobutanal revealed by one-photon mass-analyzed threshold ionization (MATI) spectroscopy", *The Journal of Chemical Physics* **2018**, *149*, 174302.

[24] C.-Y. Ng, "State-to-State Spectroscopy and Dynamics of Ions and Neutrals by Photoionization and Photoelectron Methods", *Annual Review of Physical Chemistry* **2014**, *65*, PMID: 24328445, 197–224.

Acknowledgements

Looking back over several years of my PhD studies, I realize that many people supported me and contributed to my development as a scientist and a person in general. I would like to thank everyone whom I met during this time, and in particular to those people who guided me through the complex journey of scientific research. I am deeply grateful to my supervisor Vitali Zhaunerchyk, who contributed a lot of his time to my PhD training. Vitali, your support, encouragement and comments were always very valuable for me. Without your guidance, this thesis would not have been possible. I would like to express my very great appreciation to my co-supervisor in Netherlands, Anouk M. Rijs. Thank you so much, Anouk, for your valuable training, support and suggestions. It has been a great pleasure to be a part of your group when I was in Nijmegen. I am particularly grateful to Prof. Raimund Feifel, my co-supervisor in Sweden, who was always ready to support and encourage. Thank you, Raimund, for all your advice, comments and suggestions that were very valuable.

Of course, my PhD studies would not be possible without funding organizations, therefore I would like to acknowledge Vetenskapsrådet, Sweden, and FOM Physics (NWO), The Netherlands. I would also like to thank our collaborators Prof. Michael Schmitt, Prof. Klavs Hansen, Tim Gorn, Peter Salén, Ruslan Chulkov, Prof. Stefano Stranges, Luca Schio, Robert Richter and Michele Alagia for sharing their experience. I am also grateful to Prof. Mats Larsson and Prof. Jos Oomens for valuable discussions.

I am also very thankful to people with whom I was able to work at FELIX Laboratory, especially to Daniël Bakker for his introduction to the experimental techniques at FELIX. Special thanks to Sjors Bakels, Sander Lemmens, Kasper van Lohuizen, Martijn van der Made, Jonathan Martens, Arghya Dey, Qin Ong, Daniël Rap, Lisanne Kempkes, Sebastiaan Porskamp, Mart Greuell and Nikolas Stavrias. I would also like to acknowledge the generous help and support from FELIX Laboratory staff, especially Britta Redlich, Miriam Heijmerink and Erna Gouwen; I also highly appreciate the support with technical issues, especially from Lex van der Meer, Arjan van Vliet, Bryan Willemsen, René van Buuren and Wouter Stumpel.

I would like to acknowledge the help and support of all the administrative staff at GU physics (past and present), especially

Bea Tensfeld, Marlena Härdelin, Pernilla Larsson, Maria Siirak and Clara Wilow Sundh. I am also very grateful to Jan-Åke Wiman, Mats Rostedt, Di Lu and Ranim Mallat for their assistance with different matters in the lab.

I am very thankful to Vitali, Raimund, Richard Squibb and Ranim Mallat for their valuable suggestions on how to improve the text of this thesis, and Åke Andersson for his help in the translation of the swedish summary (sammanfattning).

Furthermore, I am thankful to all colleagues at the Department of Physics, and Level 8 of Forskarhuset here at GU/Chalmers, for interesting discussions about science or everything else, for creating a stimulating and encouraging working environment, and for the nice coffee time during Friday fika, of course! I am especially grateful to Ranim, Jonas, Omid, Richard, Andreas, Dimitris, Mykola, Roman and Ludi.

Also, I would like to acknowledge Steve Gunn, Sunil Patel and Vel who contributed to the LaTeX template class available at *www.latextemplates.com*, that was used in preparing this thesis.

I would like to also take the opportunity to thank Prof. Vladimir Ya. Gayvoronsky, the supervisor of my bachelor and master internships in Ukraine. Thank you for your guidance and support on my first steps in scientific research.

And finally, I am deeply grateful to all the members of my family, who encouraged and believed in me, especially Anna and Sofia, Oleksandr and Raisa, Inna and Vitali, Halyna, Radion and Maksat. Anna, I cannot even express how grateful I am for all your support and love during all these years. Thank you for devoting a large part of your time to our little Sofia, covering her with your precious love. Thank you for backing me up when I had to finish writing yet another paper. And, thank you for bringing joy into every day of my life.

Paper I

Aminophenol isomers unraveled by conformer-specific far-IR action spectroscopy

Reproduced from
[Phys. Chem. Chem. Phys., **18**, pp. 6275-6283 (2016)]
with permission from the PCCP Owner Societies

Paper II

Far-infrared Amide IV-VI spectroscopy of isolated 2- and 4-Methylacetanilide

Reprinted from
[J. Chem. Phys. 145, 104309 (2016)]
with permission of AIP publishing

Paper III

Infrared Action Spectroscopy of Low-Temperature Neutral Gas-Phase Molecules of Arbitrary Structure

Paper IV

Conformational preferences of isolated glycylglycine (Gly-Gly) investigated with IRMPD-VUV action spectroscopy and advanced computational approaches

Paper V

Competition between folded and extended structures of alanylalanine (Ala-Ala) in a molecular beam